Agnieszka Zlotorowicz

Electrocatalysts for medium temperature PEM water electrolysis

Thesis for the degree of Philosophiae Doctor

Trondheim, June 2013

Norwegian University of Science and Technology
Faculty of Natural Science and Technology
Department of Materials Science and Engineering

NTNU – Trondheim
Norwegian University of
Science and Technology

NTNU

Norwegian University of Science and Technology

Thesis for the degree of Philosophie Doctor

Faculty of Natural Science and Technology

Department of Materials Science and Engineering

© Agnieszka Zlotorowicz

ISBN 978-82-471-4491-6 (printed version)

ISBN 978-82-471-4492-3 (electronic version)

ISSN 1503-8181

Doctoral theses at NTNU, 2013:190

IMT-Report 2013:177

Printed by NTNU-trykk

Preface

This PhD thesis contains the result of research undertaken at the Department of Material Science and Engineering at the Norwegian University of Science and Technology during the years 2010-2013. Some of the results reported here are obtained during my secondment in 2012 at the FORTH/ICE-HT at the Department of Chemical Engineering, Patras, Greece.

The thesis consists of nine chapters. The first two chapters contain the introduction and motivation of the work with a review of the literature of water electrolysis in general and proton exchange membrane water electrolysis in particular, including some aspects of operation at high temperature. The third chapter describes the experimental techniques and the instruments employed in the research. The subsequent four chapters are written as a research articles. The final two chapters are a conclusions and suggestions for further work.

I contributed to the chapters containing original research as follows:

Chapter 4: Zirconium(IV) hydrogenphosphate as an additive in electrocatalytic layers for the oxygen-evolution reaction. All the experimental work was done by me. The writing was done by me in the collaboration with my supervisors Professor Svein Sunde and Associate Professor Frode Seland.

Chapter 5: Composite thin film iridium-niobium oxide electrocatalysts for the oxygen evolution electrode. The paper was written by me in collaboration with my supervisors. I performed all the experimental work, except for the measurements performed in the test station at FORTH/ICE-HT which were made in collaboration with Nivedita Shroti and supervised by Doctor Stylianos Neophytides and Doctor Dimitris Niakolas. The XPS data were recorded by Professor Steinar Raaen at Department of Physics, NTNU.

Chapter 5 has been accepted for publication in ECS Transactions (In Press 2013).

Chapter 6: CeO_2 as an additive for anode catalyst of IrO_2 and $Ir_xRu_yO_2$ for PEM water electrolysis. The paper was written by me with help of Professor Svein Sunde and Associate Professor Frode Seland. I performed all the experimental work except for the measurement in test station where I measured in FORTH/ICE-HT with help of Nivedita Shroti supervised by Doctor Stylianos Neophytides and Doctor Dimitris Niakolas. The XPS data was recorded by Professor Steinar Raaen.

Chapter 7: Performance of a PEM water electrolysis cell of Ir-based oxide electrodes containing Ru, Nb for oxygen evolution reaction at 150 ^{o}C. The paper was written by me with contributions from Professor Svein Sunde and Associate Professor Frode Seland. The catalysts were synthesised by me. The experimental work performed in the test station at FORTH/ICE-HT were made with the help of Nivedita Shroti and supervised by Doctor Stylianos Neophytides and Doctor Dimitris Niakolas.

Acknowledgements

Undertaking this PhD has been a truly life-changing experience for me and it would not have been possible to do without the support and guidance that I received from many people.

First of all I would like to thank my main supervisor Professor Svein Sunde for accepting me as a PhD student. I am grateful for the support, discussions and his excellent guidance during my work.

Secondly I would like to thank, Associate Professor Frode Seland who took the responsibility of co-supervising my PhD. Frode has been supportive and has given me the freedom to pursue various experiments without objection. Frode has also provided insightful discussions about the research.

Thank Doctor Luis Cesar Colmenares Rausseo from SINTEF for his enthusiasm and his unselfish hep. I would also like to thank my colleagues at the department for informative discussions and for willingly assisting me when help was needed, especially Doctor Lars-Erk Owe for help in the laboratory. Thank you May Grete Sætran, Kjell Røkke and Marthe Bjerkness for taking care and helping with practical and administrative issues. I would also like to thank Annika Eriksson-Andersson, who was my office-mate during my PhD study for both scientific and less scientific discussions.

My thanks also go out to the support I received from the collaborative work at the Department of Chemical Engineering in Patras, where Doctor Stylianos Neophytides and Doctor Dimitris Niakolas were supervised on my secondment. Nivedita Shroti is acknowledged for help to measurements at the test station.

I gratefully acknowledge the funding received towards my PhD from the Marie Curie Initial Training Networks SUSHGEN and The Research Council of Norway PhD fellowship.

Finally, I would like to thank my Mom and Sister. My hard-working Mom has sacrificed her life for my Sister and myself and provided unconditional love and care. Thank you my Mom for always believing in me and encouraging me to follow my dreams.

Summary

The main subject of this PhD thesis is the fabrication and investigation the electrochemical behaviour of anode catalysts appropriate for medium-temperature proton exchange membrane (PEM) water electrolysis (WE) operating in the range 100 ^oC through 200 ^oC. These catalysts were based on metal oxides, primarily IrO_2 and its mixtures with some other oxides, and investigated as oxygen evolution electrocatalysts. A central research challenge in this project has been to understand the interaction between the anode catalyst and the solid polymer membrane electrolyte, and clarification of temperature effects.

Phosphoric acid is known as a suitable dopant to provide proton conductivity in membranes for high temperature for PEM fuel cells (FC) and WE. However, phosphates adsorb strongly on the catalyst, ultimately leading to its deactivation. Nafion, which is usually employed in low-temperature PEMFC and PEM WE is not suitable at temperatures above approximately 100 ^oC. This is because Nafion is not mechanically stable at such temperatures. However, Nafion can be stabilised by addition of zirconium phosphate. Such membranes would be an alternative to the phosphate-based membranes provided that the zirconium phosphate does not have adverse effects on the catalytic activity of for example IrO_2. On the basis of these considerations, we showed in this work that that zirconium hydrogen phosphate does not adsorb on or otherwise adversely affect the catalyst in terms of catalytic activity. In addition we even found some indications that the composite electrodes with zirconium hydrogen phosphate and Nafion can improve the utilization of iridium oxide.

Another objective here was to synthesize and characterise novel oxides for application in high-temperature PEMWE, in order to address the more stringent stability-requirements of the higher temperature. We therefore also investigated composite oxides of iridium and niobium, of iridium and cerium, and of iridium, ruthenium and cerium.

Iridium–niobium oxides were prepared by a hydrolysis method at 500 ºC. X-ray diffraction (XRD) patterns of mixed oxides containing niobium and iridium did not show any peaks corresponding to pure niobium oxide. The cell parameters and the volume of rutile unit cell did not vary with niobium content, however, and this indicates that the oxide consists of two phases and is not a solid solution. Since no peaks corresponding to the pentoxide are present, this indicates that the particles of this phase are too small to be detected in XRD, i. e. less than some 2 nm.

Niobium oxide exhibits a pronounced effect as a catalyst additive for IrO_2 catalysts. In terms of catalytic activity addition of up to 30 mol% Nb_2O_5 to iridium oxide are acceptable, and the activity of the catalyst for the oxygen evolution reaction (OER) is still appreciable compared to iridium oxide at 80 ºC in PEM WE. The rate of the OER of 50 mol% niobium in iridium oxide is significantly lower, however, the best performance in 0.5 mol dm^{-3} H_2SO_4 at room temperature was achieved with pure IrO_2. At 80 ºC only a 60 mV increase in cell voltage at 1 A cm^{-2} was found for 10 mol% Nb_2O_5 relative to that of pure IrO_2. (All electrodes contained 2 mg of catalyst per cm^2.)

The electrochemical properties of the oxides showed that the addition of Nb_2O_5 to IrO_2 particles had a highly beneficial effect at higher temperature (80 ^{o}C). Thus lower amounts of IrO_2 can be used without appreciable loss of electrocatalytic activity, and with possibly improved anodic stability. The electrocatalyst is thus a promising candidate for the OER for proton exchange membrane (PEM) water electrolysers operating at elevated temperatures.

Iridium–cerium oxides and iridium-ruthenium-cerium oxides were prepared by a hydrolysis method with an annealing temperature of 500 ºC. Electrochemical measurements performed at room temperature indicated that the addition of CeO_2 to IrO_2 or IrO_2-RuO_2 had some beneficial, but not dramatic, effects in terms of catalytic activity. XRD patterns of cerium with iridium oxide and iridium ruthenium oxide showed only peaks compatible with the rutile structure. Ceria does not change the cell parameters, which indicates that a solid solution has not formed. Therefore, these oxides consist of separate phases.

In aqueous, acidic solution at higher temperature (80 ºC) the addition of ceria to iridium oxide particles is shown to be beneficial even with 30 mol% ceria, as compared to IrO_2. Composite electrodes with ceria improve the utilization of iridium oxide and improve anodic stability. All electrodes contained 2 mg of catalyst per cm^2. The best half-cell performance in 0.5 mol dm^{-3} H_2SO_4 at 80 ºC was achieved with $(Ir_{0.8}Ru_{0.2}O_2)_{0.2}(CeO_2)_{0.2}$, for which the current was 0.03 A cm^{-2} at 1.55 V. The current for 10 and 30 mol% of CeO_2 in IrO_2 was 0.016 A cm^{-2} both at 1.55 V. Finally the current for IrO_2 was 0.025 A cm^{-2} at the same potential.

In a PEM WE cell at 80 ºC the situation changed. The iridium-ruthenium-cerium oxide showed a slightly inferior performance in this case, and the rate of the OER is similar to IrO_2 and to the mixture of 10 mol% ceria with iridium oxide.

The last part of this work was to examine the novel oxides at medium temperature (150 ºC) in a PEM WE. The anode catalysts were deposited on black carbon paper. A Membrane based on pyridine and aromatic polyethers (TPS membrane) doped phosphoric acid was used. The cross section of the MEA before and after the experiment shows that there is a good contact between the elctrocatalyst and the membrane. However the thickness of the catalysts layer and that of the membrane after the experiments were reduced, indicating some loss of catalyst during operation. This was confirmed by an associated decrease in catalyst charge after the catalyst had been exposed to high potentials. 10 mol% niobium oxide in iridium oxide showed higher electrocatalytic activity than the intrinsic IrO_2.

Table of contents

1.Introduction……………………………………………………… 1
1.1 Thesis objectives…………………………………………… 2

2. Water electrolysis………………………………………………… 5
2.1 Basic principles of water electrolysis………………………... 5
2.2 Thermodynamics and kinetics……………………………….. 7
2.3 Alkaline Water Electrolysis………………………………….. 12
2.4 Solid Oxide Electrolysis Cell (SOEC)……………………….. 13
2.5 Proton Echange Membrane Water Electrolysis (PEMWE)….. 14
    2.5.1 Biopolar Plates………………………………………… 15
    2.5.2 Gas Diffusion Layer…………………………………… 17
    2.5.3 Solid Polymer Electrolyte Membrane………………… 18
2.6 Electrocatalysts for PEM WE………………………………… 21
    2.6.1 The oxygen evolution reaction………………………… 23
    2.6.2 Preparation of metal oxide…………………………….. 25
2.7 Preparation of MEA…………………………………………. 27

3. Methodology…………………………………………………… 29
3.1 Disc electrode (DE) ………………………………………… 29
3.2 Autoclave configuration………………………………………. 29
3.3 Electrochemical characterization in a single cell SPE electrolyzer 31
    3.3.1 Low temperature……………………………………….. 31
    3.3.2 High temperature………………………………………. 32
3.4 Cyclic voltammetry (CV) …………………………………… 33
3.5 Polarisation curves…………………………………………… 34

REFERENCES…………………………………………………… 35

4. Zirconium(IV) hydrogenphosphate as an additive in electrocatalytic layers for the oxygen-evolution reaction……………………………………………………………. 47
4.1 Abstract…………………………………………………….. 47
4.2 Introduction…………………………………………………… 48
4.3 Experimental ……………………………………………….. 50
    4.3.1 Materials and chemicals………………………………… 50
    4.3.2 Solution and electrolyte preparation…………………… 50
    4.3.3 Synthesis of iridium oxide by the hydrolysis method….. 50
    4.3.4 Preparation of iridium oxide thin-film electrode……….. 51
    4.3.5 Electrochemical measurements………………………… 52
4.4 Results and discussion………………………………………… 53
4.5 Conclusion…………………………………………………… 64

4.6 Acknowledgment…………………………………………….. 65

REFERENCES……………………………………………………. 66

5. Composite thin film iridium-niobium oxide electrocatalysts for the oxygen evolution electrode………………………………………. 69
5.1 Abstract…………………………………………………. 69
5.2 Introduction…………………………………………………... 70
5.3 Experimental ………………………………………………. 71
5.3.1 Oxide preparation……………………………………… 71
5.3.2 Preparation of the electrode…………………………… 71
5.3.3 Electrochemical measurements……………………….. 73
5.3.4 XRD measurements…………………………………… 74
5.3.5 XPS measurements……………………………………. 74
5.4 Results and discussion………………………………………. 74
5.4.1 Structural and electrical properties of $(IrO_2)_{1-x}(Nb_2O_5)_x$ 74
5.4.2 Electrochemical characterisation ……………………… 80
5.5 Conclusion…………………………………………………… 87
5.6 Acknowledgment…………………………………………….. 88

REFERENCES……………………………………………………. 89

6. CeO_2 as an additive for anode catalyst of IrO_2 and $Ir_xRu_yO_2$ for PEM water electrolysis…………………………………………… 93
6.1 Abstract……………………………………………………….. 93
6.2 Introduction…………………………………………………… 94
6.3 Experimental ………………………………………………….. 96
6.3.1 Oxide preparation………………………………………. 96
6.3.2 Electrode preparation…………………………………… 96
6.3.3 Characterisation methods………………………………. 98
6.4 Results and discussion……………………………………… 100
6.4.1 Particle size and morphology ………………………… 100
6.4.2 X-ray diffraction (XRD) analysis……………………… 100
6.4.3 X- ray photoelectron spectroscopy (XPS) analysis….. 102
6.4.4 Electrochemical characterisation in acid aqueous electrolyte…………………………………………….. 106
6.4.5 PEM water electrolysis………………………………… 110
6.5 Conclusion…………………………………………………….. 113
6.6 Acknowledgment……………………………………………… 113

REFERENCES……………………………………………………. 115

7. Performance of a PEM water electrolysis cell of Ir-based oxide electrodes containing Nb, Ta and Ru for oxygen evolution reaction at 150 °C……………………………………………………………….. 119
7.1 Abstract…………………………………………………… 119
7.2 Introduction……………………………………………….. 120
7.3 Experimental ……………………………………………… 122
7.3.1 MEA preparation…………………………………… 122
7.3.2 Preparation of PEM water electrolyser……………….. 123
7.3.3 SEM and electrochemical measurement. …………….. 124
7.4 Results and discussion…………………………………….. 125
7.4.1 SEM measurement…………………………………. 125
7.4.2 PEM water electrolysis…………………………….. 127
7.5 Conclusion………………………………………………… 130
7.6 Acknowledgment…………………………………………. 131

REFERENCES…………………………………………………... 132

8. Conclusion……………………………………………………. 137
8.1 Characterisation of zirconium(IV) hydrogenphosphate as an additive in electrocatalytic layers.................................... 137
8.2 Characterisation of iridium-niobium oxide electrocatalysts.. 137
8.3 Characterization of iridium-cerium oxide and iridium-ruthenium-cerium oxide electrocatalysts…………………… 138
8.4 Performance of a PEM water electrolysis cell of Ir-based oxide electrodes containing Nb, Ta and Ru with TPS membrane at 150 ºC………………………………………… 139

9. Suggestions for further work…………………………………. 141
9.1 Development of electrocatalysts…………………………… 141
9.2 Development of the cell for the autoclave…………………. 142
9.3 PEM water electrolysis cell………………………………… 142

Acronyms………………………………………………………. 143

Errata…………………………………………………………… 144

Chapter 1

Introduction

Hydrogen is an important chemical element in the industrialized part of the world and finds uses in petrochemical industries, in electronics, and in metallurgy as a general reducing agent. There is also an increasing interest in hydrogen as a potential fuel for in alternative energy systems based on renewables, for example for use in automotive traction. In the world today approximately 40 million tons of hydrogen is produced per year, four per cent of which are produced by water electrolysis, the balance from fossil sources [1, 2]. At present, 49 per cent of the fossil-derived hydrogen is produced by reforming natural gas, 29 per cent by coal.

However, these fossil sources are limited, and the production of hydrogen from them inherently associated with emission of contaminants, such as CO and CO_2. Also, the use of fossil sources as fuels themselves would release CO_x, carbon black, heavy metals, ash, tars and organic compounds. Today's concerns about air pollution, energy security and climate change, leads to a search for new, environmentally friendly, economically attractive, and commonly accessible and renewable energy sources.

As for hydrogen as a fuel, the most universally available source is certainly water. Extracting hydrogen from water by the expenditure of electrical energy is well established, and the technique is known as electrolysis. Switching from hydrogen production from fossil fuels to water electrolysis could dramatically reduce urban air pollution, reduce the build-up of expensive greenhouse gases that threaten to trigger severe climate changes and reduce the availability of oil as a fuel in the transportation market. However, extraction of the hydrogen requires a significant input of electrical energy, currently some 4.2 kWh m^{-3} H_2 for commercial units. Also, investment costs may not be moderate. It therefore becomes important to seek ways of reducing all these input factors, for example by designing electricity-lean devices.

In principle three different technologies are available for water electrolysis (WE): alkaline water electrolysis (AWE), solid-polymer electrolyte electrolysis (SPE WE, or polymer-electrolyte membrane electrolysis– PEM WE), and (SOEC) [3-5]. Alkaline water electrolysis is the dominating technology because of the lower cost of production and since it is a well-established technology. Typically, alkaline units are operated at temperatures around 80 ^oC. PEM water electrolysis, on the other hand, may offer advantages like improved energy efficiency, higher production rate, purer hydrogen, and a more compact design [6-8]. PEM technology is also usually employed at around 80 ^oC. As detailed later in this thesis, one way to reduce the energy consumption is to increase the operating temperature of the electrolyser system. Therefore, by increasing the temperature of PEM units, to, say, 150 ^oC, one may hope to improve the performance even further. SOEC technology operates at high temperatures such as 800 ^oC, and offers a significant reduction in consumption of electrical energy, but usually requires a source of high-temperature heat. Electrolysis by SOEC is not a very mature technology.

Electrolysis of water has had, and still has, a minimal impact as an energy conversion process. This is, however, currently attracting more and more interest.

1.1 Thesis objectives

The aim of this project is to contribute to reducing the electrical energy requirements and electrolyser costs by investigating new materials for electrodes and membranes in PEM electrolysers operating at elevated temperatures. Since a major seat of loss in the electrolysers is the anode, this has been at the focus of our efforts.

One part of this project has been dedicated to the synthesis and characterization of suitable anode materials. IrO_2 was chosen as a base material for the electrocatalyst, which is expensive but highly stabile and relatively active as an oxygen evolution catalyst. To reduce the cost and improve stability and/or activity new oxides were included, and binary and ternary oxides synthesised. The study includes investigations of the electrochemical behaviour of the anode catalysts under the operating conditions of a high-temperature PEM water electrolyser. A second part of the research has been to understand the interaction between the catalyst and membranes relevant for operation at elevated temperatures.

Chapter 2

Water electrolysis

It is not quite clear who first discovered water electrolysis, and it is difficult to give the correct answer since this was done more than two hundred years ago. However, Trasatti and De Levie came to the conclusion that the phenomenon of electrolysis was first discovered in 1789 by two Dutch scientists Jan Rudolph Deiman and Adriaan Paets van Troostwijk, whereas Nicholson and Carlisle were the first who observed the phenomena the water decomposition [9, 10]. By 1902 more than 400 industrial water electrolysers were in operation [11]. The hydrogen production increased very quickly, but was crowded out by hydrogen from fossil sources in some industries in the 1950's.

In 1966, the first solid polymer electrolyte system (SPE/PEM) was built by General Electric. Almost 10 years later the first solid oxide water electrolysis cells were developed [11].

2.1 Basic principles of water electrolysis

Water electrolysis is the electrochemical splitting of water into the gases hydrogen and oxygen. An electrical power source is connected to two electrodes, the anode and the cathode which is usually (e. g. in AWE) placed in water containing an electrolyte. On the negatively polarised electrode–the cathode-hydrogen evolves. On the positively polarised electrode–the anode-oxygen evolves. In proton exchange membrane PEM water electrolysis the electrodes are attached to the membrane, which is capable of shuttling ions, typically protons, between the electrodes. The electrons are transported by the external circuit. In the PEM WE cathode the electrons and protons are recombined to form hydrogen. A schematic of

PEM water electrolysis is shown in Figure 1. The electrode and total reactions are given by (Eq.1-3),

$$\text{Anode}: \quad H_2O_{(l)} \rightarrow \frac{1}{2} O_{2(g)} + 2H_{(aq)}{}^{+} + 2e^{-} \tag{1}$$

$$\text{Cathode}: \quad 2H_{(aq)}{}^{+} + 2e^{-} \rightarrow H_{2(g)} \tag{2}$$

$$\text{Cell}: \quad H_2O_{(l)} \rightarrow \frac{1}{2} O_{2(g)} + H_{2(g)} \tag{3}$$

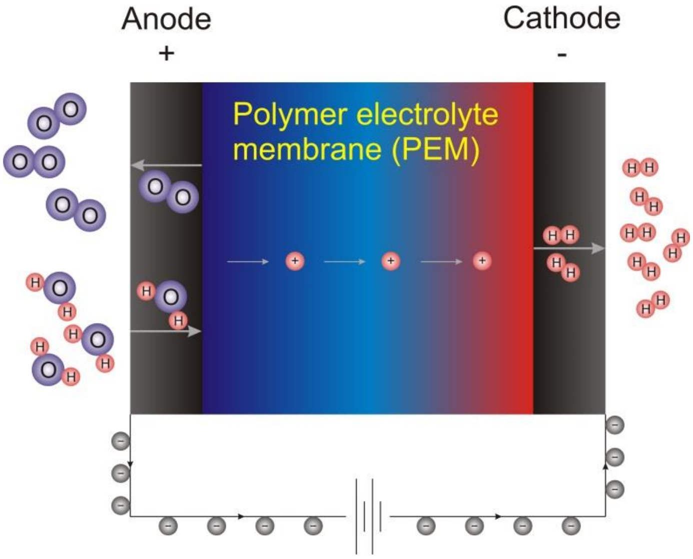

Figure 1. PEM water electrolyser schematic. The application of a voltage causes protons to move from the anode to the cathode through the proton-conductive membrane. The electrons are transported in the external circuit. On the anode oxygen is formed and on the cathode hydrogen.

2.2 Thermodynamics and kinetics

A short introduction to the thermodynamics and kinetics of water electrolysis [12, 13] will be given here.

Associated with the water-splitting reaction, Eq. (3), is a Gibbs free energy ΔG of Eq. (4)

$$\Delta G = \Delta G^0 + RT \ln\left(\frac{p_{H_2} p^{\frac{1}{2}}{}_{O_2}}{a_{H_2O}}\right) \tag{4}$$

where p is a pressure and ΔG^0 is a Gibbs free energy at standard conditions (1 atm, 25 ºC). The Gibbs free energy is the minimum (reversible) work required to split water by reaction (3). The negative of the free energy in Eq. (4) is the maximum work that can be extracted from the reverse reaction, e. g. in a fuel cell.

The reversible potential to electrochemically split water can be found using the Nernst equation (5):

$$\begin{aligned} E_{rev} &= -\frac{\Delta G}{nF} = -\frac{\Delta G^0}{nF} - \frac{RT}{nF}\ln\left(\frac{p_{H_2} p_{O_2}^{\frac{1}{2}}}{a_{H_2O}}\right) \\ &= E^0 - \frac{RT}{nF}\ln\left(\frac{p_{H_2} p_{O_2}^{\frac{1}{2}}}{a_{H_2O}}\right) \end{aligned} \tag{5}$$

where n, is the number of electrons involved in reaction (3) (n = 2), F is Faraday's constant (9.6485 x 10^4 C mol^{-1}), R is the gas law constant (8.3145 J mol^{-1} K^{-1}), E^0 is the standard potential at standard conditions (298 K, 1 atm). E_{rev} = the lowest possible applied potential between any two electrodes in order to split water.

At 298 K (25 ºC) the voltage which needs to be apply to decompose liquid water in the electrolysis cell to hydrogen and oxygen gas is 1.229 V (Table I). In addition, one needs to add an amount of heat equivalent to 0.2521 V. Hence the electrolysis requires the supply of both sufficient electrical and thermal energy is supplied.

Usually the heat required is supplied by the electrolyser itself from heat involved due to irreversible processes within the unit, such as ohmic losses and overpotentials at electrodes. These become larger the larger the voltage. The minimum voltage needed to keep the cell at constant temperature by its own action is called the thermoneutral voltage (E_{th}) and is typically 1.48 V [14].

The thermoneutral voltage is related to the enthalpy change for the process, ΔH, by, Eq.(6)

$$E_{th} = \frac{\Delta H}{nF} \tag{6}$$

When the cell potential, E_{cell}, equals the thermoneutral voltage no net heat exchange from environment takes place. For $E_{cell} < E_{tn}$, the cell absorbs heat from the outside , and when $E_{cell} > E_{tn}$ [15] the cell needs to cooled.

Liquid H_2O			
T (K)	ΔH	ΔG	TΔS
298	1.481	1.229	0.2521
373	2.469	1.167	0.3018
Vapour H_2O			
298	1.253	1.184	0.06857
373	1.257	1.167	0.0900
400	1.258	1.160	0.09799

Table I. Enthalpies of free energies of liquid and water vapour [16]

Conventional water electrolysers operate voltages exceeding 1.481 V by far in order to accommodate internal resistance and overvoltage as the system is operated at practical current densities. At finite current densities an overpotential η both for the anode and for cathode is necessary. The overpotential is defined as the difference between the actual potential (a function of the current density) and the equilibrium potential. The overpotential is an expression of the voltage-dependent part of the activation energy for the electrode reactions. An additional energy is necessary to drive the ionic migration process and overcome the resistance of the membrane, to drive electrons through the current collectors and in the balance of the internal electrical circuitry [17]. This extra energy requirement is known as the ohmic drop, iR_{cell}, within the cell. The E_{cell} potential can be written as equation (7).

$$E_{cell} = E_{anode} - E_{cathode} + \Sigma\eta + iR_{cell} \tag{7}$$

where i is the current density through the cell and R_{cell} is the sum of electrical resistances of the cell. The sum of overpotentials includes the cathode and the anode.

The overpotential of the anode and cathode, and the ohmic loss increases with current density. It can be regarded as causes of inefficiencies in the electrolysis whereby electrical energy is degraded into heat. This must be taken into account in any consideration of energy balance for electrolyser systems. Usually the degree to which the overpotentials and the ohmic losses contribute to changes in the cell voltage with potential are well separated in current-voltage diagrams. The activation losses (overpotentials) tend to increase the voltage significantly at the lower current densities, due to their logarithmic dependence on the current density (see below). Ohmic drops are usually more significant at higher current densities.

The Gibbs free energy and the enthalpy of the reaction are shown as a function of temperature in Fig. 2. Equations (8) and (9) give the efficiencies at 25 ºC. Because there will always losses present the values of Faradic efficiency are always less than one.

While the thermal efficiency can be higher than one provided the water electrolysis operates under a voltage lower than the thermo-neutral voltage. As was mentioned before, this phenomenon is due to the absorption of heat from the outside. When the denominator in Eq. (9) is 1.48 V, the electrolysis operates thermoneutrally. No heat will be absorbed from or released to the environment. The advantage of electrolysis under these thermoneutral conditions is that no auxiliary systems needed for handling the heat transport (usually cooling). This simplifies system design and reduces unit cost.

$$\eta_{Faradic} = \frac{E_{\Delta G}}{E_{cell}} = \frac{\Delta G}{\Delta G + Losses} \tag{8}$$

The thermal efficiency is defined through the enthalpy change for the water decomposition reaction,

$$\eta_{Thermal} = \frac{E_{\Delta H}}{E_{cell}} = \frac{\Delta H}{\Delta G + Losses} \tag{9}$$

The two common ways of improving the energy efficiency are increasing the operating temperature and/or pressure, or improve the components of the unit. The latter may be pursued through better membranes with higher conductivities and more active catalytic materials.

Anodic and cathodic overpotentials and the ohmic losses all vary with the current density. The overpotential is frequently given by the Tafel equation,

$$\eta_{cathode} = \ln 10 \cdot \frac{RT}{\alpha F} \log \frac{i}{i_0} \tag{10}$$

where i_0, is the so-called exchange current density of the reaction.

The Tafel equation can be derived for high overpotentials from the Butler-Volmer equation for redox reactions. For electrocatalytic reactions, which involve adsorption of intermediates at the electrode surface, the full set of equations is more complicated. However, if a rate-determining step is assumed it is frequently possible to express the resulting current-voltage behaviour as a Tafel equation. The Tafel slope $\ln 10 \cdot \frac{RT}{\alpha F}$ would then contain information regarding the rate-determining step, although not always unambiguously. The overpotential for oxygen evolution reaction (EOR) is also frequently possible to express through the Tafel equation.

For a given (electrocatalytic) reaction the exchange current density is a function of the nature of the cathode. The value of the exchange current density is critical for the performance of an electrocatalyst. The parameter α is a charge transfer coefficient, and is also a principle parameter determining the electrocatalytic activity.

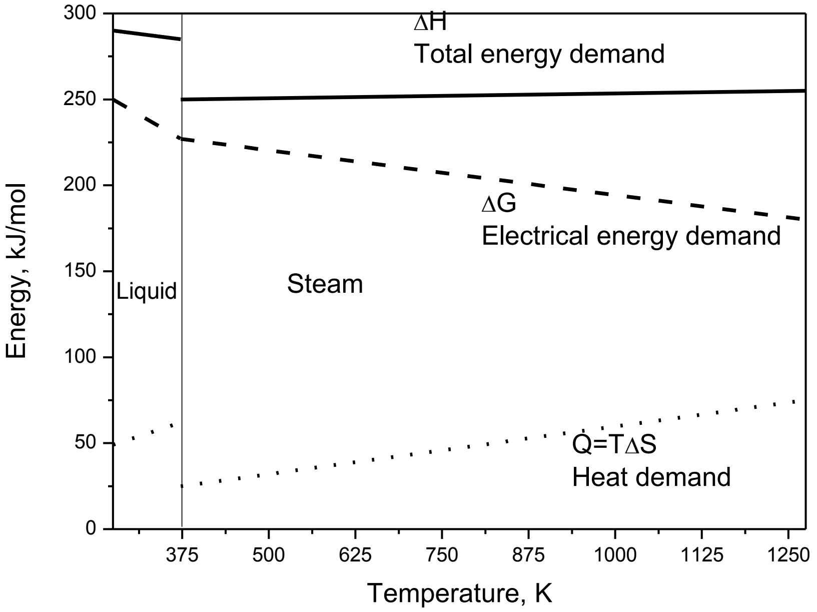

Figure 2. Energy required for water electrolysis. Increasing the temperature to above 100 ºC (373 K) increases the heat demand but reduces the electrical energy required. The total energy required is lower at high temperature than at lower, but does not include the heat required to raise the temperature in the incoming water or vapour.

2.3 Alkaline Water Electrolysis

Alkaline Water Electrolysis (AWE) is one of the technologies to produce hydrogen on a large scale from renewable energy. Commercial electrolysers use an aqueous 14-15 wt% NaOH or 25-30 wt% KOH [18, 19]. Typical operation temperatures are between 70-90 °C. Maximum operating temperatures up to 120 ºC and 40- 47 wt% KOH concentration [19] or even 250 ºC 42 bar [20] has been reported. Alkaline water electrolysers cell are either unipolar or bipolar [21]. A unipolar 'tank-type' is a single cell or tank, partially filled with electrolyte, contains a number of electrodes stack together in parallel. Both sides of each sheet of electrode material carries current of the same sign and carries out a single electrode process, i.e. oxygen or hydrogen evolution. The electrolyser can be operated with large total currents per cell by including a large number of electrodes in the cell tank. The biggest advantages of the tank-type design are simplicity of construction, a robust design, and cheap repair or replacement of malfunctioning elements. However, there are also disadvantages. The major disadvantages of tank-type electrolysers are their inability to operate at high temperatures because of heat losses from the large surface areas and the difficulty of designing the tanks to operate at high pressures.

Bipolar (filter press type) is the second type of alkaline electrolyser. The construction is similar to the tank -type design, but in this case a metallic separator between the anode and cathode is included so that the electrodes are connected in series. The gaps between the anodes and cathodes can be made very narrow, and this reduces the ohmic drop in the electrolyte. To separate the evolving gases the anode and cathode compartments are separated by a membrane. The bipolar system is more compact and lightweight. However, it is a more complicated of construction. Bipolar electrolysers can be operated under pressure [19], in contrast to the unipolar cells.

Materials in the alkaline electrolysers need to be highly corrosion resistant. Asbestos has been extensively used as cell separator [22]. Its use is now prohibited in more than 40 countries, including all EU countries [23]. It could be replaced advantageously by synthetic materials like polysulfones or oxide ceramic materials like nickel oxide [24], calcium tiatnate [25], nickel alloyed with molybdenum [26].

There are few companies which are producing hydrogen by alkaline electrolysis technology, DeNora, Hydrogenics and Lurgi and Norsk Hydro (now incorporated to Statoil) in Norway which is the world leader.

2.4 Solid Oxide Electrolysis Cell (SOEC)

SOECs operating at high temperature consumes less electrical energy and is more efficient for hydrogen production compared with the ordinary alkaline water electrolysis [27, 28]. This is a very interesting concept since as temperature increases a higher proportion of the total energy required to electrolyze water can be supplied by thermal energy instead of electricity as was described in Chapter 2.2. Moreover, the power and heat generated by nuclear power systems and renewable energy sources, and waste heat from high temperature industrial processes can be utilized for steam electrolysis in SOECs [29, 30]. From the thermodynamic viewpoint of water decomposition, it is more advantageous to electrolyze water at high temperature (800-1000 ^{o}C) because the energy is supplied in mixed form of electricity and heat. The main advantage is that a substantial part of the energy needed for the electrolysis process is added as heat, which is much cheaper than electric energy. The electrical energy decreases with increasing temperature as shown in figure 2. In addition, the high temperature accelerates the reaction kinetics, reducing the energy loss due to electrode polarization, thus increasing the overall system efficiency [31-33]. At 100 ^{o}C the ratio of ΔG to ΔH is 93 % where at temperature 1000 ^{o}C is about 70 % [34]. The early solid oxide cell was developed by Dornier-system GmbH [34], and is currently experiencing renewed interest.

The solid oxide cells are connected in series and consist of gas-tight cylindrical electrolyte and porous anode and cathode electrodes [35]. It is a similar structure only with a reverse operation of solid oxide fuel cell (SOFC). Steam is dissociated at the cathode side of the solid structure where it is reduced into hydrogen, the oxygen ions are transported through the ceramic material to the anode, where they discharge and form oxygen gas, releasing electrons.

The reported study about SOECs is mainly based on the research in SOFCs (Solid Oxide Fuel Cells), including cell fabrication, stack and electrodes and electrolyte materials [36-38]. The electrolyte layer is sandwiches between anode and cathode. The most commonly used SOEC consists of strontium doped lanthanum manganite (LSM)-yttria-stabilized zirconia (YSZ) composite as oxygen electrode and YSZ as the electrolyte [30, 39, 40]. In the LSM-YSZ anode electrode, LSM provides electrochemical activity for oxygen ions (O^{2-}) oxidation and electronic conductivity, while YSZ provides ionic conductivity and improves the adhesion between the LSM-YSZ electrode and the YSZ electrolyte. Wang et al. [41] tested different composite electrodes of yttria-stabilised zirconia (YSZ) with $LaSrMnO_3$ (LSM), strontium doped lanthanum $LaSrFeO_3$ (LSF), and $LaSrCoO_3$ (LSCo) as anodes. Ni cermet (Ni+YSZ) for the cathode [34].

Typical high temperature electrolyser such as the German HOT ELLY system achieves 92 % electrical efficiency while low temperature electrolysers can reach at most 85 % efficiency.

2.5 Proton Exchange Membrane Water Electrolysis (PEM WE)

In the more recent years, the proton exchange membrane (PEM) water electrolysers have developed into a commercially available technology. PEM water electrolysers were developed at General Electric Company (USA) in 1966 for fuel cell, and later, electrolyser applications [42].

The central piece of a PEM electrolyser is the solid polymer, proton-conducting membrane. An assembly of the membrane, two dispersed catalyst layers on either side of it, and two gas diffusion layers (GDL) is commonly referred to as a membrane electrode assembly (MEA). As it shown in Figure 3 a complete PEM WE cell is then comprised of three types of components: a membrane electrode assembly (MEA) and two bipolar with channels for gas flowing (flow field or separator) plates, and eventually two seals. The catalytic layer of the anode consists of a blend of noble metal oxides (e.g. RuO_2 and IrO_2) and the polymer, while the catalytic material of the hydrogen electrode (cathode) is Pt metal usually supported on carbon. The outline of reactions and the associated transport through the membrane was described in chapter 2.1.

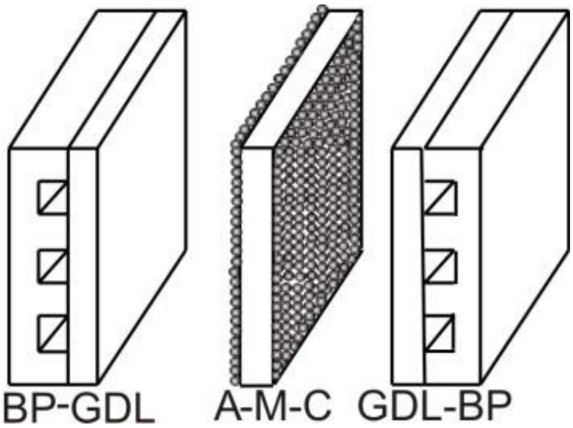

Figure 3. The membrane-electrode assembly of a PEM water electrolyser. BP-bipolar plate, GDL: Gas diffusion layer and current collector, A: Anode catalyst layer, M: Membrane and C: Cathode catalyst layer. In a stack the catalyst layer would be homogenous on both sides.

2.5.1 Bipolar Plates

The bipolar plates in PEM fuel cell stacks contributes significantly to both cost and weight of the PEM WE, and account for about 80% of total weight and 40% of the costs [43, 44].

The most common plates are made from corrosion resistant metal and non-porous machined graphite sheets, but the process to fabricate them is very expensive and time-consuming [44]. Alternative materials are therefore being actively pursued, such as stainless steel [45-48], aluminium, nickel or titanium [49], and coated metals coated. To avoid corrosion, metallic bipolar plates are typically coated with protective layers. Coatings should be conductive and adhere to the base metal without exposing it. Two types of coatings, carbon-based and metal-based, have been investigated. Carbon-based coatings include conductive polymer [43], diamond-like carbon [43] and organic self-assembled monopolymers [43]. Gold coating [50], chromium nitride [51] were also tried. The bipolar plates typically have six functions [49, 52]:

(1) to separate the individual cells in the stuck
(2) to carry current away from the cell
(3) to remove heat from the active areas
(4) to prevent leakage of reactants
(5) to facilitate water management within the cell
(6) to distribute the fuel and oxidant within the cell.

For a material to qualify for bipolar plates, Borup and Vanderborgh [43] and Mehta and Cooper [49] have suggested the following criteria/properties: electrical conductivity, plate resistance, thermal conductivity, hydrogen/gas permeability, corrosion resistance, compressive strength and density.

The flow of the water can be controlled by employing different patterns in the bipolar plates. The bipolar plates have different designs to improve a gas flow by avoiding the trapping of bubbles in the channels which reduce the overall active area. There are, in principle, four different types of flow fields [53] that have been investigated in the past:

- pin-type [54, 55]
- series-parallel channels [56]
- serpentine [57, 58]
- integrate [59, 60]
- interdigitated [61]

The pin-type flow field has many pins arranged in a regular pattern. These pins are usually cubical or circular in cross-section. This type of flow field design entails the gas flow field plate having a number of parallel flow channels which are also connected to the gas inlet and exhaust. The serpentine flow field has the channels arranged linear and parallel to another, but creates a multiple of mini-serpentine flow path. The serpentine flow field is the most widely used design in industry. Chow et al. [59] designed the integrate flow field which possesses both reactant gas flow field and cooling flow field on the same plate surfaces, it shown in the ref. [53]. The interdigitated flow field is the modification of the integrate flow and is described in more details in ref. [53].

2.5.2 Gas Diffusion Layer (GDL)

Proton exchange membrane water electrolysis and/or fuel cells require anode and cathode catalyst layers that have good electronic contact with current collectors. These current collectors are called gas diffusion layers (GDLs), which are critical components in achieving high performance in the PEM WE. The GDL influences the transport of the reactant gas to the catalyst layer and removes liquid water from the gas channels, conduct electrons with low resistance and preferably have a low contact resistance to the various interfaces [62]. The bipolar plate and the current collectors as a cell component are held together under high compressive loads to prevent gas leakages. Gas leakages cause poor performance, while over-compressing the GDL increases mass transfer resistance and thus reduces cell performance. High contact pressure can decrease the contact resistance and it has been shown that physical compression of the gas diffusion layer directly increases its electrical conductivity [63, 64].

The GDL is fabricated by either porous carbon materials (e.g., carbon cloth or carbon fiber paper or their modification) [65-67], or metals (e.g. Ti) [68] or gold plated porous titanium sinters. [69].

Carbon materials like Toray Paper, Sigracet, and Freudenberg gas diffusion layer are lightweight, cheap, and have a small volume. However, at high temperatures or potentials they react easily with active oxygen species. The anode will then corrode due to the formation of carbon monoxide or carbon dioxide. The carbon GDL will quickly be consumed, which will then leave a physical gap that will give a very poor electrical contact to the Membrane Electrode Assembly (MEA). This all means that the electrolyser will essentially stop operating, or at the very least operate at very poor inefficiencies. The anode GDL should be electronically conductive, corrosion resistant, non-ion leaching and allow easy transport of water to the membrane and active sites and simple gas release from the electrode structure.

Metallic diffusion layers have a high resistance toward corrosion. However, they would still form oxidized layers at their surfaces, and these will increase the resistance of the metallic diffusion layer during water electrolysis. To avoid this oxidation new gas layers diffusion like platinised titanium screen have been fabricated. These consist of thin titanium screens coated with a thin layer of platinum.

However, also some new carbon materials are being developed. A novel micro-protective layer (MPL) coated on a carbon-made gas diffusion layer is invented to combine these two devices and test on a novel device to improve the original defects [70-72].

2.5.3 Solid Polymer Electrolyte Membrane

The proton exchange membrane water electrolysis is based on the use of a polymeric proton exchange membrane as the solid electrolyte and was first proposed by General Electric for fuel cell, and later, electrolyser applications. The proton exchange membrane electrolyser technology was developed by ABB (formerly Brown, Boveri Ltd), over the years from 1976 to 1989 [42].

For low temperature the most commonly employed membrane for PEM WE is Nafion, a proton conductive polymer based on perfluorosulfonic acid and extensively employed as a membrane for PEM fuel cells. Nafion has a high protonic conductivity and a good mechanical and electrochemical stability [73, 74]. Because of its water-assisted conduction mechanism, Nafion can be used only at temperatures below 80 °C. However, to decrease the complexity and increase the efficiency, there is a strong need for PEMs capable of sustained operation above 100 °C. Unfortunately, the proton conductivity of Nafion suffers greatly at temperatures above 80 °C due to loss of water [75, 76].

Second type of solid polymer electrolyte at low temperature is SPEEK, sulfonated polyetherketone. Sulfonated aromatic high performance polymers exhibit similar domain formation and proton conductivity as Nafion at high levels of hydration [77]. However, the conductivity of the sulfonated aromatic polymers is lower at low levels of hydration and as a consequence the conductivity is significantly lower.

The operating temperature of the above mentioned membranes can be increased if materials such as inorganic oxides (i.e. SiO_2 [78-80], TiO_2 [76, 78], ZrO_2 [78, 79, 81], CeO_2 [82]), metal phosphates (i.e. ZrP, TiP) or heteropolyacids (HPA) [77, 83] are introduced in the membrane structure. Nafion polymer-based organic/inorganic composite membranes have been investigated using hydrophilic and/or proton-conducting compounds such as $Zr(HPO_4)_2$ [84-87]. Zirconium(IV) hydrogenphosphate (commonly called ZrP) as a hygroscopic insoluble salt gives improvement in performance under dehydrating conditions. ZrP was the desired additive to Nafion-based membranes because of its attributes as described by Hogarth et all [88]. ZrP is a Brønsted acid with an ability to donate protons, increase the mobility of protons in its surface and thus the conductivity. It has a good electrochemical stability and good chemical stability in water, which allows its long term use above 130 ºC. A molecular sieve-type of structure, with constricted pores, enhances the ability for water transport. The water uptake improves the mechanical stability and ionic interaction with Nafion and increases the glass transition temperature, which is helpful for operation at higher temperatures.

Holdcroft et al. [85] thus found out that addition of zirconium phosphate nanoparticles into Nafion membranes decreased the dimensional stability of the composite membranes upon swelling with water. Also, ZrP affected the water retention, water permeation and proton transport. The water content increased with increasing ZrP for low ZrP contents (<20 wt.-%), but decreased at higher ZrP content (>20 wt.-%) (Figure 4).

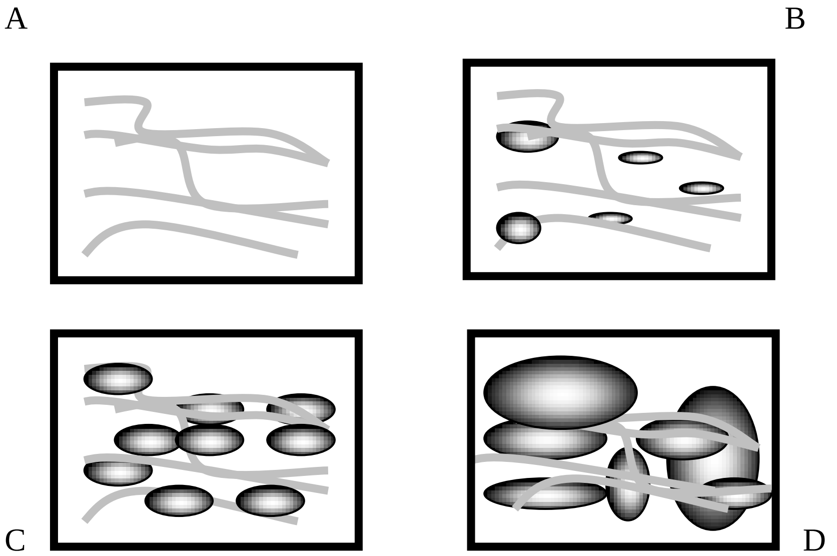

Fugure 4. Structure of nanoparticles of ZrP inside Nafion fibers. The grey lines correspond to Nafion membrane structure, where the oblate ellipsoid inorganic black object is the ZrP [89].The examples show different wt% of ZrP in Nafion: A: 0 wt% , B: <10 wt%, C: 10<wt% ZrP<20, D: wt% ZrP> 20. Reproduced with permission from [85].

This transition is attributed to ZrP particles, increasing in size as ZrP content increased until 20 wt.-%. At ZrP content > 20 wt.-%, they no longer fit inside the hydrophilic pores of Nafion. In this case ZrP disrupts the proton-conducting pathway in the membranes resulting in a lowering of proton mobility and proton conductivity.

Sacca et al. developed composite membranes containing different percentages of ZrO_2 and tested in the temperature range of 80-130 ºC [81]. Antonucci et al. found that a composite Nafion-SiO_2 membrane for SPE electrolysers showed promising properties for high temperature up to 120 ºC. They suggested that this effect is mainly due to a significantly better water retention than the bare Nafion [80]. Park et al. [90] developed composite membranes containing different Zr:Si mole ratios in a Zr-O_2-SiO_2 binary oxide. This binary oxide was found to be effective in improving proton conductivity and water uptake at high temperatures at 120 ºC and low humidity 50 % RH.

Recent reports showed that Nafion/PTFE (NF) (PTFE-porous poly(tetrafluoro ethylene) membranes are cheap, they have a good mechanical strength in both swollen and unswollen state, they have a good thermo-stability, and they are thinner. Silicate-hybridized NF and zirconium phosphate hybridized NF have proved higher conductivity and better PEMFC performance than Nafion [91].

For higher temperature the alternative membrane is PBI polymer- poly[2,2'-(m-phenylene)-5,5'-bibenzimidazole], which has a high-proton conductivity and excellent mechanical properties [92]. However, PBI membranes need to be doped with highly concentrated phosphoric acid to achieve a sufficient conductivity [93]. The first patent was filed by Savinell and Litt [94]. High conductivity, good mechanical properties and thermal stability have been reported at temperatures up to 200 ºC under ambient pressure [95, 96]. Chemically, PBI is a basic polymer and can readily react with a strong acid. Various inorganic acids have been investigated such as H_3PO_4 [95, 97], H_2SO_4 [95, 98], $HClO_4$ [99], HNO_3 [99], HBr [95], HCl [99]. Phosphoric acid is of special interest because of its high proton conductivity, also under anhydrous conditions, as well as its excellent thermal stability and very low vapour pressure at elevated temperatures [100].

Alternatively, pyridine containing poly(ether sulfone), which has a high molecular weight, excellent mechanical properties as well as thermal and oxide stability [101], and PTFE [90], as support materials for Nafion [91] or PBI [102] were applied in high temperature fuel cells and might find application in PEM water electrolysis as well.

2.6 Electrocatalysts for PEM WE

In the process of hydrogen production by water electrolysis, most of the over-potential that gives rise to losses is related to the electrochemical process at the anode, where the oxygen evolution reaction takes place [103]. Much effort has been spent on improving the anodic activates and this reaction and mechanism is not widely understood.

A good catalyst needs to have high surface area and electrical conduction, good electrocatalytic properties, long-term mechanical and chemical stability, minimal gas bubble problems, enhanced selectivity, availability and low cost and health safety [104]. After 1965, when Henry B. Beer obtained his patent on the dimensionally stable anode (DSA) [105], oxides of Ru have been used for many years as a prototype of DSA. Catalyst that makes more efficient use of these metals is frequently being sought by adding a second component by improving selectivity and stability by synergetic action [106, 107]. Active oxides like IrO_2 and RuO_2 are mixed with the inert oxides of the valve metal group TiO_2, ZrO_2, Ta_2O_5, Nb_2O_5 or with various purposes e.g. SnO_2, CeO_2 [107].

Although not extensively investigated in this area, catalyst architecture may play a role as well. Some possible structures are displayed in Figure 5. The structure in Figure 5a is simply mono dispersed particles (most likely nano sized) solid solution. Fig. 5b is monodispersed particles in two separated phases.

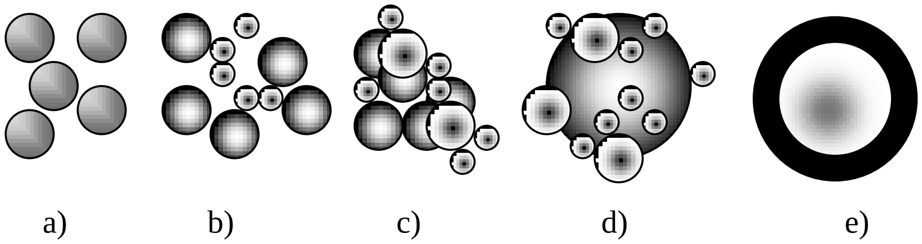

Figure 5. Binary oxide catalyst structures: a) monodisperesd oxide solid solution, b) monodispersed oxide with separated phases, c) agglomeration of the catalyst, d) active catalyst decorated with inert oxide, e) core-shell structure, with an inert oxide in the core and the catalyst on the shell.

Agglomerates particles are illustrated in Figure 5c, the particles should be porous to have high surface area and active sites. The next figure 5d shows a structure with small inert particles attached to the catalyst, or nano-particles decorating a larger support particle. The second option enables a very high active area. The last structure, 5e, is a more recently investigated structure, characterised a high active surface area and improved utilisation of the expensive component. The structure is referred to as a core- shell structure. The inert or less active oxide or metal is a core and the shell is the active particle.

2.6.1 The oxygen evolution reaction

The OER is strongly dependent on the catalyst, and although no single, generally accepted mechanism is available, the reaction is generally assumed to involve adsorbed intermediates. The following mechanism may serve as an example [108]. The first step is a charge transfer step with the formation of an adsorbed hydroxyl species on the active site- S.

$$S + H_2O \rightarrow S\text{-}OH_{ads} + H^+ + e^- \qquad (14)$$

The second step is a second charge transfer step that deprotonates the adsorbent:

$$\text{S-OH}_{ads} \rightarrow \text{S-O}_{ads} + \text{H}^+ + \text{e}^- \qquad (15)$$

The next step is the formation of an oxygen molecule and the back-formation of two active sites:

$$S\text{-}O + S\text{-}O \rightarrow 2S + O_{2(g)} \qquad (16)$$

Various correlations between catalytic activity and adsorption have been formulated. These are usually base on some variety of the Sabatier principle, according to which the interaction between the substrate and a reaction intermediate should be neither too strong nor too weak. An interaction that is too weak will be inefficient because the substrate will fail to bind the intermediate species. The reaction will take place only at a slow pace, and reaction (14) becomes rate limiting. On the other hand, if the interaction is too strong, the catalyst gets blocked by the adsorbent, that fails to desorb, and reaction (15) or (16) become rate-limiting. This complex combination of reactions involving surface species and material transformations has led to the representation of kinetic information in so-called Volcano plots [109, 110]. The Sabatier principle implies that a catalyst with an optimum strength of the interaction between the catalyst and the substrate will give the maximum reaction rate.

An example of a Volcano plot is given in Figure 6, in which the enthalpy of transition from a lower oxide to a higher oxide is taken to represent the binding energy of adsorbents. IrO_2 and RuO_2 reside near the apex of the volcano, as indicated above.

Metal oxides react with water and become covered by protons or OH-groups, depending on pH, which determine the interfacial properties of the oxide surface in the solution such as the point of zero charge. Water molecules are adsorbed onto the metal cation while a proton from molecules of water becomes transferred to a neighboring oxygen atom in the oxide lattice. Metal ions of high electronegativity withdraw electrons from the OH-groups, which dissociated and the metal oxide acts as an acid. Metal ions of low electronegativity tend to push electrons into the OH group, on the other hand, the M-OH bonds become weak, and the metal oxide acts as a base [104]. The catalytic activity of oxides has therefore also been reported to correlate with the pzc [111, 112].

Other ions than protons and hydroxyl groups may adsorb on the oxide and interfere with the electrochemical reactions there. Thus Kazarinov and co-workers identified the adsorption of anions on RuO_2 by means of a radiotracer technique [113].

Tamura et al. [114] have worked with Cl^- and they have found an anomalous E-pH dependence explained in terms of surface complex formation. F^- ions which are not specifically adsorbed on metals, interact very strongly with a hydrophilic surface of oxides [115]. The following order of increasing degree adsorption has been established [116, 117]: $ClO_4^- \ll Cl^- < HSO_4^- < H_2PO_4^-$. Adsorption obeys a logarithmic isotherm for uniformly inhomogeneous surfaces and is reversible for all ions except $H_2PO_4^-$ [116].

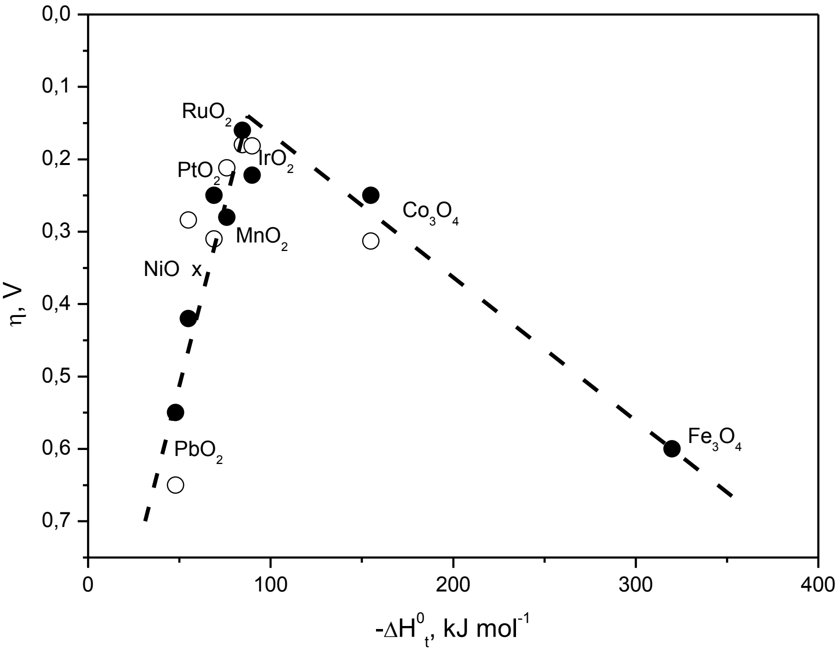

Figure 6. Electrocatalytic activity towards the oxygen evolution reaction of various oxides as a function of the enthalpy of the lower to higher oxide transition, in acid (○) and alkaline (●) solutions, (Reproduced from [104])

Adsorption studied as a function of composition of the active layer which was described by Andreev [116]. This group have found that in the RuO$_2$-TiO$_2$ oxide TiO$_2$ is also active in anion adsorption. This means that the properties of the Ru sites are affected by the neighbouring sites and by Ti site too.

2.6.2 Preparation of metal oxides

DSA electrode layers are normally formed by direct decomposition of noble precursor (typically chlorides) onto the metallic supports.

Electrocatalysts for PEM water electrolysis electrodes are often synthesised first and then formed into the MEA. Synthesis of metal oxides for PEM WE is frequently performed by wet chemical methods, like hydrolysis, polyol or sol-gel. The hydrolysis method [118, 119] is the most often used technique in the NTNU group. A metal hydroxide is formed by reacting the metal precursor, typically a salt like hexachloroiridic acid, with an aqueous sodium hydroxide solution. This results in ligand exchange. The resulting hydroxo, aquo-hydroxo, or oxy-hydroxo complexes then form the metal oxide through inorganic condensation reactions [120]. The produced powder catalyst is heated in an oxygen-containing atmosphere in a furnace during which crystallisation will result to a degree depending on temperature and duration [121]. An advantage of this method is for example the ability to fabricate anhydrous RuO_2 by heating hydrous RuO_2 at various temperatures [122].

In the polyol method [123] nanosize noble metal colloids of for example platinum, iridium or ruthenium are produced by the reduction of metal precursors in ethylene glycol [124]. The polyol acts as both as a solvent and a reducing agent [125]. A significant advantage of the polyol method is that one can control the particle size and thus obtain nano-sized particles by decreasing the reaction time and by increasing the nucleation rate. Wang et al. suggested for example that the particles size can be controlled by adding a H_2O to the synthesis solution [126]. Changing the pH of the metallic colloid-polyol mixture also affects the agglomeration process of the colloid [127].

Sol-gel method is based on the process of transforming a liquid-based sol into a solid gel phase. Oxide particles and oxide coating layers on the substrate can be obtained. Murakami et al. [128] worked on the binary oxide like IrO_2-SeO_2, ternary oxides. SnO_2-IrO_2-Ta_2O_5 was prepared by Ardizzone [129].

In the sol-gel method referred to as the Pechini method, also called the polymeric precursor method (PPM), metal citrates are polymerized using ethylene glycol. This involves the polymerisation of the metal citrate monomers by condensation. Layers somewhat similar to DSA electrode layers can be produced. The polymer gel that forms has metal ions homogeneously distributed through it. The gel is then calcined to form the metal oxide. For example, dissolving $RuCl_3xH_2O$ in citric acid /ethylene glycol mixture produces an ester, the calcination of which leads to ruthenium oxide. Terezo et al. [130] synthesised Ti/IrO_2–Nb_2O_5 by similar means.

The Adams fusion method is another method that can be employed to synthesize oxides relevant for PEM WE. Heat treatment is used to convert hydroxide particles to oxide. A molten salt like $NaNO_3$ is the oxidation agent [131]. The Adams fusion method has been employed to produce IrO2 [132, 133], and mixed oxides such as $Ir_xRu_{1-x}O_2$ [133-135], IrO_2-Ta_2O_5 [136], $Ir_{0.4}Ru_{0.6}Mo_xO_y$ [137], $Ir_xPt_{1-x}O_2$ [138] and SnO_2-RuO_2-IrO_2 [132, 139], $Ru_xSn_{1-x}O_2$ [139] powders from their precursor salts for PEM water electrolysis applications.

2.7 Preparation of MEA

The catalytic layers of the PEM WE anode consist of a blend of the catalyst (noble metal oxides, e.g. IrO_2) and an ionomer. The catalytic material of the hydrogen electrode–the cathode-is Pt supported on carbon.

There are two modes of MEA assembly: (1) application of an ink containing polymers and electrocatalytic particles to the GDL followed by membrane attachment or (2) vice versa, the application of the catalyst layer to the membrane followed by GDL attachment. These methods are widely used for fuel cells and water electrolysis. The ink can be applied on to the porous support material (CCS-catalyst coated substrate) or on to the membrane (CCM-catalyst coated membrane) by airbrush spraying, brush, screen printing or by the “doctor-blade” technique.

The spraying technique has the advantages of simplicity and the relatively precise control of catalyst loading compared to the other methods.

In the spraying method described by Srinivasan et al.[141], the electrolyte is suspended in a mixture of water, alcohol, and colloid PTFE. This ink is ultrasonically mixed and then repeatedly sprayed onto wet-proofed carbon paper or membrane. Rasten [134] used a mixture of electrocatalysts particles, 5 wt% Nafion, water, ethanol and glycerol. In order to speed up the drying of the ink during deposition, highly volatile solvents like ethanol are normally used, while glycerol is added to improve the homogeneity of the membrane (due to a higher viscosity) [142]. In addition, the membrane (or electrode) is fixed on a hot plate at 80 ºC during the spraying process.

The second technique is painting. In the painting method described by Gottesfeld, Wilson and Zawodzinski [143], an ink of water, isopropanol, PTFE and catalyst particles are ultrasonically mixed. The method is similar to spraying, but instead of an airbrush a paint brush is used. A layer of ink is painted directly onto a membrane or carbon cloth on a heated vacuum table. The bulk of the solvent is removed at a lower temperature to alleviate cracking and the final traces of solvent are rapidly removed at higher temperatures.

A third method is the catalyst decaling method, again described by Gottesfeld, Wilson and Zawodzinski [143]. Catalysts are deposited on to the membrane using a "decal" process in which the ink (dissolved Nafion, electrocatalyst powder, water and glycerol to get the desired viscosity of the ink) is cast onto PTFE blanks for transfer to the membrane by hot pressing. When the PTFE blank is peeled away, a thin casting layer of catalyst is left on the membrane.

The last method to be described here is a dry application to the membrane or the porous support material as described by Gulzow et al. [144]. Reactive materials (Pt/C, PTFE, PFSA powder and/or filler materials) are mixed in a knife mill. The mixture is then atomized and sprayed in a nitrogen stream through a slit nozzle directly onto the membrane. The layer is fixed by hot rolling or pressing. The process is simple, and the fundamental idea for this process is to spray a dry catalytic layer directly onto membrane to avoid waiting times for evaporating solvents and to accomplish a good contact between the catalytic layer and the electrolyte membrane. Layers as thin as 5 μm have successfully been obtained by this method.

Chapter 3

3. Methodology

This section describes some of the more central methods and equipment employed, including autoclave measurements which was partly established during this work, the electrochemical methods and some details of the normalisation of the electrochemical measurements. Standard characterisation methods such as XRD will not be included, as the reader is referred to the general literature.

3.1 Disc electrode (DE)

In a separate three-electrode setup operating at room temperature only, a Pine instruments glassy carbon (GC) electrode disc electrode (DE) was used as the support material for the electrocatalyst and acted as the working electrode (0,19625 cm^2 geometric surface area). A high-area Pt sheet sealed in glass was used as the counter electrode and a dynamic hydrogen electrode as the reference electrode. The electrolyte used in all experiments was 0.5 mol dm^{-3} H_2SO_4 (Sigma- Aldrich, 95–97%), electrolyte. The DE was mechanically polished, previously by α-micro polish alumina 5.0 microns, washed carefully with Milli-Q water and then it was polished with γ micro polish deagglomerated alumina 0.05 microns and washed with distilled water and degreased with isopropanol.

3.2 Autoclave configuration

A standard three electrode set-up was implemented in an autoclave (150 ml Miniclave steel, Büchi Glas Uster AG) allowing for temperatures up to 200 °C and 10 bars. The electrolyte used in all experiments was 0.5 mol dm^{-3} H_2SO_4 electrolyte. A Pt sheet sealed in glass was used as the counter electrode and a reversible hydrogen electrode in the same electrolyte (0.5 mol dm^{-3} sulphuric acid) functioned as the reference electrode. Ohmic drop was minimized by placing the reference Luggin in as close to the working electrode surface as practically possible. The working electrode consisted of an MEA with only one electrode deposited and mounted in a custom made glass pipe (Figure 7) facing the reference electrode compartment. The active electrodes were prepared by spraying an ink containing the electrocatalyst and Nafion ionomer in isopropanol directly to Nafion 115 membranes (N-115, Ion Power Inc.) at 80 ºC using a argon driven air brush (Badger 360G) .

The geometric electrode area was 2 cm^2 with an electrocatalyst loading of 2 mg oxide cm^{-2} and a Nafion content within the electrocatalytic layer of 5 wt% attached to one side of a piece of Nafion membrane. The active side of the membrane electrode assembly was mounted next to a gold mesh (for even current distribution) and PEEK sinters (diameter 16 mm, thickness 4 mm), which allowed for electronic contact to the oxide electrode surface. The membrane side of the MEA was facing the inner compartment of the glass pipe allowing for separate electrolyte compositions. When run with equal electrolyte, the counter electrode was placed in the reference electrode compartment. The experiments were performed in a temperature window of 20- 120 ºC. A BioLogic SAS Potentiostat Model VMP3 was used to control the potential between the reference and the working electrode and measure the current in the working and counter electrode circuit.

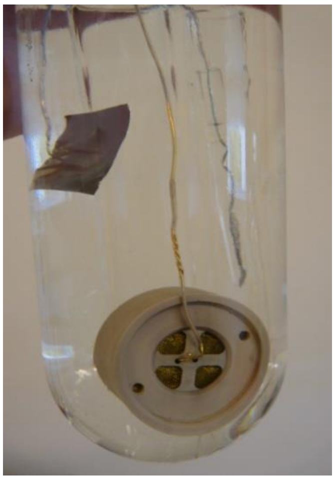

Figure 7. Electochemical glass autoclave cell with three electrodes: MEA- working electrode, Pt- sheet -counter electrode and RE- reference electrode in the Luggin probe. The gold wire is the current collector.

3.3 Electrochemical characterization in a single cell SPE electrolyzer

A single-cell test station was employed for in-situ assessment of performance of the PEM WE catalysts and MEAs. The cells for low temperature characterization were based on Nafion, while phosphoric-acid doped membrane based on pyridine and aromatic polyethers (TPS membranes) were used for measurements at higher temperatures. Custom made Poco Graphite Blocks with single serpentine flow field patterns were used as bipolar plates. The anode block was gold coated to prevent vigorous corrosion of the carbon bipolar plate. The cell surface area was 5 cm^2. A Princeton Applied Research Potentiostat/Galvanostat Model 263 was used to control the potential at the working electrode versus the hydrogen reference electrode.

3.3.1 Low temperature

The PEM water electrolysis test cell was used to evaluate the performance of the synthesised materials by employing the oxide catalyst mixture as the anode catalyst, and 30% Pt/C (30% Pt on Vulcan XC-72R, E-TEK Inc.) as the cathode catalyst. The membrane electrode assembly (MEA) was prepared by the catalyst covered membrane (CCM) technique by brushing both sides of a piece of Nafion (Fumapem F-10120 supplied from Fumatech, thickness 110-130 µm). The ink was prepared by ultrasonicating a mixture of electrocatalyst and Nafion (acting as a binder and electrolyte in the catalytic layers) in an appropriate amount of isopropanol/water (1:1) as solvent. The ink was then applied to a piece of membrane fixed on a vacuum table held at 75 ºC. The active geometric electrode surface area was 4.84 cm^2 and the electrocatalyst : 5wt% Nafion solution : isopropanol/water - ratio was fixed to 1:8:15 for both cathode and anode. The cathode loading was approximately 1.5 mg Pt cm^{-2} and the anode loading about 5 mg oxide cm^{-2}. The MEA was mounted between two carbon fibre papers supplied by Freudenberg (Freudenberg FCCT KG, type H2315 C2). Deionised water passes through the cell with helium gas acting as carrier gas with a steady flow of 100 cc min^{-1}. The oxides were electrochemically characterized at three temperatures; 20, 60 and 80 ºC, and repeated twice. Deionised water was circulated at 0.15 ml min^{-1}.

3.3.2 High temperature

The PEM water electrolysis test cell used to evaluate the performance of the synthesised materials at high temperature was similar to that employed at lower temperature. Again the cell was made by applying the metal oxide as the anode catalyst and 30% Pt/C (30% Pt on Vulcan XC-72R, E-TEK Inc.) as the cathode catalyst. However, the anode electrode was now prepared by the catalyst coated surface (CCS) technique by depositing the catalytic ink with spatula onto the wet-proofed carbon paper (Freudenberg FCCT KG, H2315 C2). The loading at the anode was about 10 mg oxide cm^{-2} and was estimated from the difference in weight of the carbon paper before and after the deposition. The anode electrode was dried overnight at room temperature before weighing. The active area of the prepared electrode was 4 cm^2.

A TPS membrane (thickness ~120-130 μm, Advent, Greece) was prepared as the polymer electrolyte membrane for MEA preparation at high temperature. Before use, the membranes were pretreated in 85 % H_3PO_4 at 140 °C for overnight. The doping level was approximately 200 %.

The cathode electrocatalytic ink was supplied by ADVENT and contained phosphoric acid (2 g 85 % orto-phosphoric acid, Sigma- Aldrich). This ink was mixed well and sprayed onto one side of the TPS membrane. A piece of carbon cloth plain (CCP20, Fuel Cell Earth)) was employed as the gas diffusion layer and mechanical support at the cathode.

Deionised water passes through the cell with argon gas with 100 cc min^{-1} flow. The oxides were measured at 150 °C. Deionised water was circulated at 0.15 ml min^{-1}.

3.4 Cyclic voltammetry (CV)

In cyclic voltammetry the electrode potential is scanned at constant sweep rate between two potential limits, and the current response arising from the reactions occurring at the electrode is monitored as a function of the potential. In linear sweep voltammetry, the potential is scanned from one potential to another, and the experiment is halted. In cyclic voltammetry the potential returns to the initial potential after reaching the peak potential.

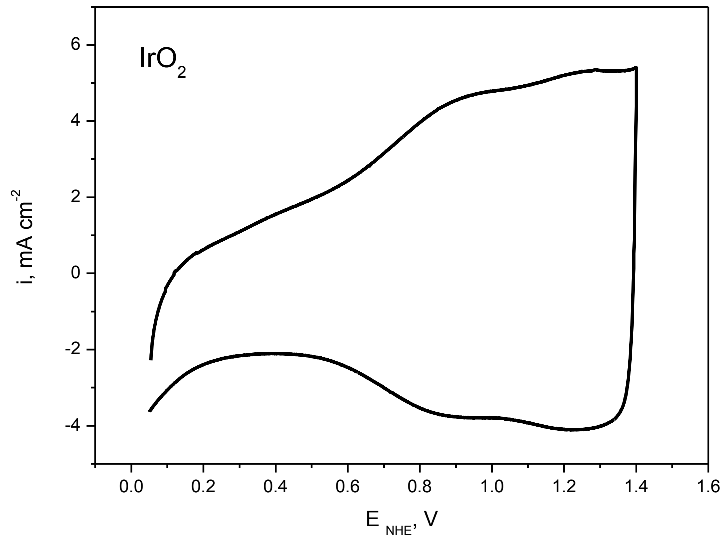

Figure 8. Voltammogram of an IrO_2, hydrolysis method, 0.5 mol dm^{-3} H_2SO_4 (200 mV s^{-1})

A typical voltammogram of IrO_2 in sulphuric acid is shown in Figure 8. The voltammogram shows the solid-state redox transitions of the oxide as peaks, or in this case as rather broad waves. These redox transitions correspond to the intercalation (cathodic currents) and expulsion (anodic currents) of protons in the oxide. The intercalated species thus store charge in the oxide. The two anodic and cathode peaks apparent in the voltammogram of iridium oxide in acid are located around 0.8-0.9 and 1.25-1.35 V and correspond to the redox transitions of Ir^{3+}/Ir^{4+} and Ir^{4+}/Ir^{6+}, respectively.

3.5 Polarisation curves

Due to gas evolution at the electrode surface, we found it difficult to obtain steady currents at constant potential, as would normally be used for recording polarisation curves. Therefore slow linear sweep voltammetry was used as a compromise. The sweep rate was always 5 mV min^{-1}.

To compare two or more electrodes it is necessary to somehow assess the true surface area of the catalyst. For oxides of the type studied here this is usually done based on voltammetric charge. Thus, a series of cyclic voltammetry with different of sweep rates were recorded to integrate the current potential curve. This makes it possible to find the so-called inner, outer and total charge of the electrode. At high sweep rates, the outer charge dominates and the total charge at low the sweep rates. In the latter case the intercalation species have time to go to very deep into the oxide and the diffusion layer has time to relax to its equilibrium state before the sweep returns. Quantitatively the outer charge can be found by plotting the integrate charge q^* vs. the inverse of the square root of the seep rate $1/\sqrt{\nu}$. Extrapolating the curve to zero ($\nu \rightarrow \infty$) gives the outer charge. The total charge is found by plotting $1/q^*$ vs. $\sqrt{\nu}$ and extrapolating the resulting straight line to zero ($\nu \rightarrow 0$) gives the total charge. More details are given by Ardizzone et al. in Ref. [145]

Reference

1. http://www.iea.org/.
2. http://www.freedoniagroup.com/brochure/26xx/2605smwe.pdf, 2010
3. R.L. LeRoy, Industrial water electrolysis: Present and future. *Int. J. Hydrogen Energ.*, **8**(6) (1983) 401-417.
4. H. Takenaka, E. Torikai, Y. Kawami, N. Wakabayashi, and T. Sakai, Studies on solid polymer electrolyte in water electrolysis. 1. Some properties of Nafion- exchange membranes as a solid polymer. *Denki Kagaku*, **52**(6) (1984) 351-357.
5. U. Guth and H.H. Mobius, Studies on water- vapor eøectrolysis with solid electrolyte cells conducting oxide ions. *Zeitschrift Fur Chemie*,. **16**(6) p. 249 (1976).
6. S.A. Grigoriev, V.I. Porembsky, and V.N. Fateev, Pure hydrogen production by PEM electrolysis for hydrogen energy. *Int. J. Hydrogen Energ.*, **31**(2) (2006) 171-175.
7. S.A. Grigoriev, P. Millet, and V.N. Fateev, Evaluation of carbon-supported Pt and Pd nanoparticles for the hydrogen evolution reaction in PEM water electrolysers. *J. Power Sources*, **177**(2) (2008) 281-285.
8. S.A. Grigoriev, P. Millet, S.V. Korobtsev, V.I. Porembskiy, M. Pepic, C. Etievant, C. Puyenchet, and V.N. Fateev, Hydrogen safety aspects related to high-pressure polymer electrolyte membrane water electrolysis. *Int. J. Hydrogen Energ*, **34**(14) (2009) 5986-5991.
9. S. Trasatti, Water electrolysis: who first? *J. Electroanal. Chem.*, **476** (1999) 90-91.
10. R. de Levie, The electrolysis of water. *J. Electroanal. Chem.*, **476** (1999) 92-93.
11. W. Kreuter and H. Hofmann, Electrolysis: the important energy transformer in a world of sustainable energy. *Int. J. Hydrogen Energ*. **23 (**1998) 661−666.
12. D. Plecher, R. Greef, R. Peat, L.M. Peter, and J. Robinson, Instrumental methods in electrochemistry. Woodhead Publishing, Chichester, 2001.
13. A.J. Brad and L.R. Faulkner, Electrochemical methods: Fundamentals and applications. Wiley, New York, 2001.
14. F.J. Salzano, G. Skaperdas, and A. Mezzina, Water vapor electrolysis at high temperature: Systems considerations and benefits. *Int. J. Hydrogen Energ.* **10**(12) (1985) 801-809.
15. R.L. LeRoy, C.T. Bowen, and D.J. Leroy, The Thermodynamics Of Aqueous Water Electrolysis. *J. Electrochem. Soc.*, **127**(9) (1980) 1954-1962.

16. J.R. Elliott and M. Gleiser, Thermochemistry for Steel-making. Addison- Wesley, Reading, Massachusetts, 1: p. 176. 1960
17. K. Zeng and D. Zhang, Recent progress in alkaline water electrolysis for hydrogen production and applications. Prog.Energ. Comb. Sci., **36**(3) (2010) 307-326.
18. J. Kerres, G. Eigenberger, S. Reichle, V. Schramm, K. Hetzel, W. Schnurnberger, and I. Seybold, Advanced alkaline electrolysis with porous polymeric diaphragms. Desalination, **104**(1–2) (1996) 47-57.
19. H. Vandenborre, R. Leysen, H. Nackaerts, D. Van der Eecken, P. Van Asbroeck, W. Smets, and J. Piepers, Advanced alkaline water electrolysis using inorganic membrane electrolyte (I.M.E.) technology. *Int. J. Hydrogen Energ.*, **10**(11) (1985) 719-726.
20. F. Allebrod, C. Chatzichristodoulou, and M.B. Mogensen, Alkaline electrolysis cell at high temperature and pressure of 250 °C and 42 bar. *J. Power Sources*, **229**(0) (2013) 22-31.
21. D. Stolten and K. D., Hydrogen and Fuel Cells. Fundamentals, Technologies and applications. Alkaline Electrolysis-Introducyion and Overview. WILEY-VCH Verlag GmbH&Co. KGaA,: p. 256, 2010
22. P. Godin, R. Graziotti, A. Damien, and P. Masniere, Asbestos corrosion study in a caustic potash solution at several temperatures. *Int. J. Hydrogen Energ.*, **2**(3) (1977) 291-297.
23. WHO, Elimination of Asbestos-related Diseases. 2006.
24. D.E. Hall, Alkaline Water Electrolysis Anode Materials. *J. Electrochem. Soc.*, **132**(2) (1985) 41C-48C.
25. R.W. Vine and S.T. Narsavage, Porous matrix structures for alkaline electrolyte fuel cells. *Electrochem. Soc. Extended Abstr.*, **75** (1975) 96.
26. I.A. Raj and K.I. Vasu, Transition metal-based hydrogen electrodes in alkaline solution - electrocatalysis on nickel based binary alloy coatings. *J. App. Electrochem.*, **20**(1) (1990) 32-38.
27. K.H. Quandt and R. Streicher, Concept and design of a 3.5 MW pilot plant for high temperature electrolysis of water vapor. *Int. J. Hydrogen Energ*, **11**(5) (1986) 309-315.
28. Z. Zhan, W. Kobsiriphat, J.R. Wilson, M. Pillai, I. Kim, and S.A. Barnett, Syngas production by coelectrolysis of CO 2/H 2O: The basis for a renewable energy cycle. *Energ.Fuels*, **23**(6) (2009) 3089-3096.
29. C.M. Stoots, J.E. O'Brien, K.G. Condie, and J.J. Hartvigsen, High-temperature electrolysis for large-scale hydrogen production from nuclear energy - Experimental investigations. *Int. J. Hydrogen Energ*, **35**(10) (2010) 4861-4870.

30. M. Ni, M.K.H. Leung, K. Sumathy, and D.Y.C. Leung, Potential of renewable hydrogen production for energy supply in Hong Kong. *Int. J. Hydrogen Energ*, 2006. **31**(10): p. 1401-1412.
31. M. Ni, M.K.H. Leung, and D.Y.C. Leung, Technological development of hydrogen production by solid oxide electrolyzer cell (SOEC). *Int. J. Hydrogen Energ*, **33**(9)(2008) 2337-2354.
32. J.D. Holladay, J. Hu, D.L. King, and Y. Wang, An overview of hydrogen production technologies. *Catal. Today*, **139**(4) (2009) 244-260.
33. J.E. O'Brien, C.M. Stoots, J.S. Herring, and J. Hartvigsen, Hydrogen production performance of a 10-cell planar solid-oxide electrolysis stack. *J. Fuel Cell Sci.Tech*., **3**(2) (2006) 213-219.
34. R. Hino, K. Haga, H. Aita, and K. Sekita, 38. R&amp;D on hydrogen production by high-temperature electrolysis of steam. *Nucl. Eng. Des.*, **233**(1–3) (2004) 363-375.
35. J. Udagawa, P. Aguiar, and N.P. Brandon, Hydrogen production through steam electrolysis: Model-based steady state performance of a cathode-supported intermediate temperature solid oxide electrolysis cell, *J. Power Sources*, **166**(1) (2007) 127-136.
36. Z. Wang, M. Mori, and T. Araki, Steam electrolysis performance of intermediate-temperature solid oxide electrolysis cell and efficiency of hydrogen production system at 300 Nm3 h-1. *Int. J. Hydrogen Energ.,* **35**(10) (2010) 4451-4458.
37. J.E. O'Brien, C.M. Stoots, J.S. Herring, P.A. Lessing, J.J. Hartvigsen, and S. Elangovan, Performance measurements of solid-oxide electrolysis cells for hydrogen production. *J. Fuel Cell Sci. Tech.*, **2**(3) (2005) 156-163.
38. J.S. Herring, J.E. O'Brien, C.M. Stoots, G.L. Hawkes, J.J. Hartvigsen, and M. Shahnam, Progress in high-temperature electrolysis for hydrogen production using planar SOFC technology. *Int. J. Hydrogen Energ.*, **32**(4) (2007) 440-450.
39. S.H. Jensen, P.H. Larsen, and M. Mogensen, Hydrogen and synthetic fuel production from renewable energy sources. *Int. J. Hydrogen Energ*, **32**(15) (2007) 3253-3257.
40. A. Brisse, J. Schefold, and M. Zahid, High temperature water electrolysis in solid oxide cells. *Int. J. Hydrogen Energ*, **33**(20) (2008) 5375-5382.
41. W. Wang, Y. Huang, S. Jung, J.M. Vohs, and R.J. Gorte, A comparison of LSM, LSF, and LSCo for solid oxide electrolyzer anodes. *J. Electrochem. Soc.,* **153**(11) (2006) A2066-A2070.
42. P. Millet, D. Dragoe, S. Grigoriev, V. Fateev, and C. Etievant, GenHyPEM: A research program on PEM water electrolysis

supported by the European Commission. *Int. J. Hydrogen Energ,* **34**(11) (2009) 4974-4982.

43. R.L. Borup and N.E. Vanderborgh. Design and testing criteria for bipolar plate materials for PEM fuel cell applications. 1995.
44. H. Tsuchiya and O. Kobayashi, Mass production cost of PEM fuel cell by learning curve. *Int. J. Hydrogen Energ,* **29**(10) (2004) 985-990.
45. D.P. Davies, P.L. Adcock, M. Turpin, and S.J. Rowen, Stainless steel as a bipolar plate material for solid polymer fuel cells. *J. Power Sources*, **86**(1) (2000) 237-242.
46. D.P. Davies, P.L. Adcock, M. Turpin, and S.J. Rowen, Bipolar plate materials for solid polymer fuel cells. *J. App. Electrochem*., **30**(1) (2000) 101-105.
47. H. Wang and J.A. Turner, Ferritic stainless steels as bipolar plate material for polymer electrolyte membrane fuel cells. *J. Power Sources*, **128**(2) (2004) 193-200.
48. H. Wang, M.A. Sweikart, and J.A. Turner, Stainless steel as bipolar plate material for polymer electrolyte membrane fuel cells. *J. Power Sources*, **115**(2) (2003) 243-251.
49. V. Mehta and J.S. Cooper, Review and analysis of PEM fuel cell design and manufacturing. *J. Power Sources*, **114**(1) (2003) 32-53.
50. S.J. Lee, C.H. Huang, J.J. Lai, and Y.P. Chen, Corrosion-resistant component for PEM fuel cells. *J. Power Sources*, **131**(1-2) (2004) 162-168.
51. M.P. Brady, K. Weisbrod, I. Paulauskas, R.A. Buchanan, K.L. More, H. Wang, M. Wilson, F. Garzon, and L.R. Walker, Preferential thermal nitridation to form pin-hole free Cr-nitrides to protect proton exchange membrane fuel cell metallic bipolar plates. *Scripta Materialia*, **50**(7) (2004) 1017-1022.
52. A. Hermann, T. Chaudhuri, and P. Spagnol, Bipolar plates for PEM fuel cells: A review. *Int. J. Hydrogen Energ*, **30**(12) (2005) 1297-1302.
53. X. Li and I. Sabir, Review of bipolar plates in PEM fuel cells: Flow-field designs. *Int. J. Hydrogen Energ*, **30**(4) (2005) 359-371.
54. C.A. Reiser and R.D. Sawyer, Solid polymer electrolyte fuel cell stack water management system. US Patent No. 4,769,297, 1988.
55. C.A. Reiser, Water and heat management in solid polymer fuel cell stack. US Patent No. 4,826,742, 1989.
56. A. Pollegri and P.M. Spaziante, US Patent No. 4,197,178,, 1980.
57. F.R. Spurrier, B.E. Pierce, and M.K. Wright, US Patent No. 4,631,239, , 1986.
58. J.S.J. Granata and B.M. Woodle, US Patent No. 4,684,582, 1987.

59. C.Y. Chow, B. Wozniczka, and J.K.K. Chan, Integrated reactant and coolant fluid flow field layer for a fuel cell with membrane electrode assembly. Canadian Patent No. 2,274,974, 1999.
60. C.Y. Chow, US Patent No. 5,804,326, 1998.
61. A. Kazim, H.T. Liu, and P. Forges, Modelling of performance of PEM fuel cell with conventional and interdigitated flow fields. *J. Appl. Electrochem*., **29** (1999) 1409-1416.
62. B. Thoben and A. Siebke, Influence of different gas diffusion layers on the water management of the PEFC cathode. *J. New Mater. Electrochem. Syst*., **7** (2004) 12-20.
63. J. Ihonen, F. Jaouen, G. Lindbergh, and G. Sundholm, A novel polymer electrolyte fuel cell for laboratory investigations and in-situ contact resistance measurements. *Electrochim. Acta*, **46**(19) (2001) 2899-2911.
64. J. Ge, A. Higier, and H. Liu, Effect of gas diffusion layer compression on PEM fuel cell performance. *J. Power Sources*, **159**(2) (2006) 922-927.
65. K. Darowicki and J. Orlikowski, Impedance Investigations of the Mechanism of Oxygen Evolution on Composite Electrodes. *J. Electrochem. Soci.*, **146**(2) (1999) 663-668.
66. F. Marangio, M. Pagani, M. Santarelli, and M. Calì, Concept of a high pressure PEM electrolyser prototype. *Int. J. Hydrogen Energ*., **36**(13) (2011) 7807-7815.
67. L.A. Da Silva, V.A. Alves, M.A.P. Da Silva, S. Trasatti, and J.F.C. Boodts, Oxygen evolution in acid solution on IrO_2 + TiO_2 ceramic films. A study by impedance, voltammetry and SEM. *Electrochim. Acta*, **42**(2) (1997) 271-281.
68. E. Rasten, G. Hagen, and R. Tunold, Electrocatalysis in water electrolysis with solid polymer electrolyte. *Electrochim. Acta*, **48**(25-26) (2003) 3945-3952.
69. A.T. Marshall and R.G. Haverkamp, Production of hydrogen by the electrochemical reforming of glycerol–water solutions in a PEM electrolysis cell. *Int. J. Hydrogen Energ*, **33**(17) (2008) 4649-4654.
70. Y.N. Zhang, H.M. Zhang, Y.W. Ma, J.B. Cheng, H.X. Zhong, S.D. Song, and H.P. Ma, A novel bifunctional electrocatalyst for unitized regenerative fuel cell. Journal of Power Sources, 2010. **195**(1): p. 142-145.
71. S. Altmann, T. Kaz, and K.A. Friedrich, Bifunctional electrodes for unitised regenerative fuel cells. *Electrochim. Acta*, **56**(11) (2011) 4287-4293.
72. C.-Y. Liu, L.-H. Hu, and C.-C. Sung, Micro-protective layer for lifetime extension of solid polymer electrolyte water electrolysis. *J. Power Sources*, **207**(0) (2012) 81-85.

73. M. Saito, N. Arimura, K. Hayamizu, and T. Okada, Mechanisms of ion and water transport in perfluorosulfonated ionomer membranes for fuel cells. *J. Phys. Chem. B*, **108**(41) (2004) 16064-16070.
74. A. Siu, J. Schmeisser, and S. Holdcroft, Effect of water on the low temperature conductivity of polymer electrolytes. *J. Phys. Chem. B*, **110**(12) (2006) 6072-6080.
75. L.A. Neves, J. Benavente, I.M. Coelhoso, and J.G. Crespo, Design and characterisation of Nation membranes with incorporated ionic liquids cations. *J. Mem. Sci*., **347** (2010) 42-52.
76. V. Baglio, R. Ornelas, F. Matteucci, F. Martina, G. Ciccarella, I. Zama, L.G. Arriaga, V. Antonucci, and A.S. Arico, Solid Polymer Electrolyte Water Electrolyser Based on Nafion-TiO_2 Composite Membrane for High Temperature Operation. *Fuel Cells*, **9**(3) (2009) 247-252.
77. K.D. Kreuer, On the development of proton conducting materials for technological applications. *Sol. St. Ion*., **97**(1-4) (1997) 1-15.
78. N.H. Jalani, K. Dunn, and R. Datta, Synthesis and characterization of Nafion (R)-MO2 (M = Zr, Si, Ti) nanocomposite membranes for higher temperature PEM fuel cells. *Electrochim. Acta*, **51**(3) (2005) 553-560.
79. K. Li, G. Ye, J. Pan, H. Zhang, and M. Pan, Self-assembled Nafion®/metal oxide nanoparticles hybrid proton exchange membranes. *J. Mem. Sci*., **347**(1–2) (2010) 26-31.
80. V. Antonucci, A. Di Blasi, V. Baglio, R. Ornelas, F. Matteucci, J. Ledesma-Garcia, L.G. Arriaga, and A.S. Aricò, High temperature operation of a composite membrane-based solid polymer electrolyte water electrolyser. *Electrochim. Acta*, **53**(24) (2008) 7350-7356.
81. A. Sacca, I. Gatto, A. Carbone, R. Pedicini, and E. Passalacqua, ZrO2-Nafion composite membranes for polymer electrolyte fuel cells (PEFCs) at intermediate temperature. *J. Power Sources*, **163**(1) (2006) 47-51.
82. Z. Wang, H. Tang, H. Zhang, M. Lei, R. Chen, P. Xiao, and M. Pan, Synthesis of Nafion/CeO2 hybrid for chemically durable proton exchange membrane of fuel cell. *J. Mem. Sci*., **421–422**(0) (2012) 201-210.
83. S.M.J. Zaidi, S.D. Mikhailenko, G.P. Robertson, M.D. Guiver, and S. Kaliaguine, *J. Membr. Sci*., **173** (2000) 17-34.
84. C. Yang, S. Srinivasan, A.S. Arico, P. Creti, V. Baglio, and V. Antonucci, Composition Nafion/zirconium phosphate membranes for direct methanol fuel cell operation at high temperature. *Electrochem. Sol. St. Lett*., **4**(4) (2001) A31-A34.

85. M.P. Rodgers, Z. Shi, and S. Holdcroft, Ex situ Characterisation of Composite Nafion Membranes Containing Zirconium Hydrogen Phosphate. *Fuel Cells*, **9**(5) (2009) 534-546.
86. P. Costamagna, C. Yang, A.B. Bocarsly, and S. Srinivasan, Nafion® 115/zirconium phosphate composite membranes for operation of PEMFCs above 100 °C. *Electrochim. Acta*, **47**(7) (2002) 1023-1033.
87. H. Hou, G. Sun, Z. Wu, W. Jin, and Q. Xin, Zirconium phosphate/Nafion115 composite membrane for high-concentration DMFC. *Int. J. Hydrogen Energ.*, **33**(13) (2008) 3402-3409.
88. W.H.J. Hogarth, J.C. Diniz da Costa, and G.Q. Lu, Solid acid membranes for high temperature (¿ 140 ºC) proton exchange membrane fuel cells. *J.Power Sources*, **142**(1-2) (2005) 223-237.
89. D. Truffier-Boutry, A. De Geyer, L. Guetaz, O. Diat, and G. Gebel, Structural study of zirconium phosphate-nafion hybrid membranes for high-temperature proton exchange membrane fuel cell applications. *Macromol.*, **40**(23) (2007) 8259-8264.
90. K.T. Park, U.H. Jung, D.W. Choi, K. Chun, H.M. Lee, and S.H. Kim, ZrO2-SiO2/Nafion (R) composite membrane for polymer electrolyte membrane fuel cells operation at high temperature and low humidity. *J. Power Sources*, **177**(2) (2008) 247-253.
91. H.L. Lin, S.H. Yeh, T.L. Yu, and L.C. Chen, Silicate and zirconium phosphate modified Nafion/PTFE composite membranes for high temperature PEMFC. *J. Pol. Res.*, **16**(5) (2009) 519-527.
92. G. Qian, D.W. Smith Jr, and B.C. Benicewicz, Synthesis and characterization of high molecular weight perfluorocyclobutyl-containing polybenzimidazoles (PFCB-PBI) for high temperature polymer electrolyte membrane fuel cells. *Pol.*, **50**(16) (2009) 3911-3916.
93. J.S. Wainright, J.-T. Wang, D. Weng, R.F. Savinell, and M. Litt, Acid-Doped Polybenzimidazoles: A New Polymer Electrolyte. *J. Electrochem. Soc.*, **142**:L121-L123 (1995).
94. R. Savinell and M. Litt, Proton conducting polymers used as membranes. Case Western reserve University, US patent 5,525,436, 1996.
95. R. Bouchet and E. Siebert, Proton conduction in acid doped polybenzimidazole. *Sol. St. Ion.*, **118**(3-4) (1999) 287-299.
96. J.T. Wang, R.F. Savinell, J. Wainright, M. Litt, and H. Yu, A H2/O2 fuel cell using acid doped polybenzimidazole as polymer electrolyte. *Electrochim. Acta*, **41**(2) (1996) 193-197.
97. S. Wasmus, J.T. Wang, and R.F. Savinell, Real- time mass spectrometric investigation of methanol oxidation in a direct methanol fuel- cell. J. *Electrochem. Soc.*, **142**(11) (1995) 3825-3833.

98. M. Kawahara, J. Morita, M. Rikukawa, K. Sanui, and N. Ogata, Synthesis and proton conductivity of thermally stable polymer electrolyte: poly(benzimidazole) complexes with strong acid molecules. *Electrochim. Acta*, **45**(8-9) (2000) 1395-1398.

99. B.Z. Xing and O.J. Savadogo, The effect of acid doping on the conductivity of polybenzimidazole (PBI). *Mater. Electrochem. Sys.*, **2**(2) (1999) 95-101.

100. S.J. Paddison, K.D. Kreuer, and J. Maier, About the choice of the protogenic group in polymer electrolyte membranes: Ab initio modelling of sulfonic acid, phosphonic acid, and imidazole functionalized alkanes. *Phys. Chem*., **8**(39) (2006) 4530-4542.

101. E.K. Pefkianakis, V. Deimede, M.K. Daletou, N. Gourdoupi, and J.K. Kallitsis, Novel polymer electrolyte membrane, based on pyridine containing poly(ether sulfone), for application in high-temperature fuel cells. *Macromol. Rapid Commun*., **26**(21) (2005) 1724-1728.

102. J.P. Shin, B.J. Chang, J.H. Kim, S.B. Lee, and D.H. Suh, Sulfonated polystyrene/PTFE composite membranes. *J. Membr. Sci*., 2005. 251(1-2): p. 247-254.

103. J.O.M. Bockris, Hydrogen no longer a high cost solution to global warming: New ideas. *Int. J. Hydrogen Energ.*, **33**(9) (2008) 2129-2131.

104. S. Trasatti, Electrocatalysis in the anodic evolution of oxygen and chlorine. *Electrochim. Acta*, **29**(11) (1984) 1503-1512.

105. H.B. Beer, British Pat. no. 1,147,442,1969.

106. S. Ardizzone and S. Trasatti, Interfacial properties of oxides with technological impact in electrochemistry. *Adv. Coll. Int. Sci.*, **64**(0) (1996) 173-251.

107. R. Kötz and S. Stucki, Stabilization of RuO_2 by IrO_2 for anodic oxygen evolution in acid media. *Electrochim. Acta*,**31**(10) (1986) 1311-1316.

108. J.O.M. Bockris, Kinetics of Activation Controlled Consecutive Electrochemical Reactions: Anodic Evolution of Oxygen. *J. Chem. Phys.,* **24** (1956) 817-827.

109. A. Logadottir, T.H. Rod, J.K. Nørskov, B. Hammer, S. Dahl, and C.J.H. Jacobsen, The Brønsted–Evans–Polanyi Relation and the Volcano Plot for Ammonia Synthesis over Transition Metal Catalysts. *J. Catal*., **197**(2) (2001) 229-231.

110. S. Dahl, A. Logadottir, C.J.H. Jacobsen, and J.K. Nørskov, Electronic factors in catalysis: the volcano curve and the effect of promotion in catalytic ammonia synthesis. *App. Catal. A: Gen*., **222**(1–2) (2001) 19-29.

111. G.A. Parks and P.L. De Bruyn, The zero point of charge of oxides. *J. Phys. Chem.*, **66** (1962) 967-973.
112. G.A. Parks, The Isoelectric Points of Solid Oxides, Solid Hydroxides, and Aqueous Hydroxo Complex Systems. *Chem. Rev.*, **65** (1965) 177-198.
113. V.E. Kazarinov and V.N. Andreev, Elektrokhimiya, **14 (**1978)
114. T. Arikado, C. Iwakura, and H. Tamura, Some oxide catalysts for the anodic evolution of chlorine: reaction mechanism and catalytic activity. *Electrochim. Acta*, **23**(1) (1978) 9-15.
115. J. Sanchez and J. Augustynski, X-ray photoelectron spectroscopic study of the interaction of various anions with the oxide-covered titanium metal. *J. Electroanal. Chem. Int. Electrochem.*, **103**(3) (1979) 423-426.
116. A. Daghetti, G. Lodi, and S. Trasatti, Interfacial properties of oxides used as anodes in the electrochemical technology. *Mater. Chem. Phys.*, **8**(1) (1983) 1-90.
117. S. Ardizzone, P. Siviglia, and S. Trasatti, The point of zero charge of ruthenium dioxide. *J. Electroanal. Chem. Int.. Electrochem.*, **122**(0) (1981) 395-401.
118. A.T. Marshall, S. Sunde, M. Tsypkin, and R. Tunold, Performance of a PEM water electrolysis cell using $Ir_xRu_yTa_zO_2$ electrocatalysts for the oxygen evolution electrode. *Int. J. Hydrogen Energ.*, **32**(13) (2007) 2320-2324.
119. I.A. Lervik, M. Tsypkin, L.E. Owe, and S. Sunde, Electronic structure vs. electrocatalytic activity of iridium oxide. *J. Electroanal. Chem.*, **645**(2) (2010) 135-142.
120. J.-P. Jolivet, Metal Oxide Chemistry and Synthesis. From Solution to Solid State, John Wiley & Sons, New York. p.1-52, 2000
121. L.-E. Owe, M. Tsypkin, K.S. Wallwork, R.G. Haverkamp, and S. Sunde, Iridium–ruthenium single phase mixed oxides for oxygen evolution: Composition dependence of electrocatalytic activity. *Electrochim. Acta*, **70**(0) (2012) 158-164.
122. C. Iwakura, K. Hirao, and H. Tamura, Preparation of ruthenium dioxide electrodes and their anodic polarization characteristics in acidic solutions. *Electrochim. Acta*, **22**(4) (1977) 335-340.
123. A. Marshall, B. Børresen, G. Hagen, S. Sunde, M. Tsypkin, and R. Tunold, Iridium oxide-based nanocrystalline particles as oxygen evolution electrocatalysts. *Russ. J. Electrochem.*, **42**(10) (2006) 1134-1140.
124. L.K. Kurihara, G.M. Chow, and P.E. Schoen, Nanocrystalline metallic powders and films produced by the polyol method. *Nanostruct. Mater.*, **5**(6) (1995) 607-613.

125. C. Bock, C. Paquet, M. Couillard, G.A. Botton, and B.R. MacDougall, Size-selected synthesis of PtRu nano-catalysts: Reaction and Size Control Mechanism. *J.Amer.Chem.Soc.*, **126** (2004) 8028-8037.

126. P. Diao, D. Zhang, J. Wang, and Q. Zhang, Electrocatalytic activity of supported gold nanoparticles toward CO oxidation: The perimeter effect of gold–support interface. *Electrochem. Commun.*, **12**(11) (2010) 1622-1625.

127. A. Miyazaki, K. Takeshita, K. Aika, and Y. Nakano, Formation of ruthenium colloid in ethylene glycol. *Chem. Lett.*, (4) (1998) 361-362.

128. Y. Murakami, H. Ohkawauchi, M. Ito, K. Yahikozawa, and Y. Takasu, Preparations of ultrafine IrO2-SnO2 binary oxide particles by a sol-gel process. Electrochim. Acta, **39**(17) (1994) 2551-2554.

129. S. Ardizzone, C.L. Bianchi, G. Cappelletti, M. Ionita, A. Minguzzi, S. Rondinini, and A. Vertova, Composite ternary SnO_2–IrO_2–Ta_2O_5 oxide electrocatalysts. J. Electroanal. Chem., **589**(1) (2006) 160-166.

130. A.J. Terezo and E.C. Pereira, Fractional factorial design applied to investigate properties of Ti/IrO_2–Nb_2O_5 electrodes. *Electrochim. Acta*, **45**(25–26) (2000) 4351-4358.

131. R. Adams and R.L. Shriner, Platinum oxide as a catalyst in the reduction of organic compounds. III. Preparation and properties of the oxide of platinum obtained by the fusion of chloroplatinic acid with sodium nitrate. *J. Am. Chem. Soc.*, **45**(9) (1923) 2171-2179.

132. R. Hutchings, K. Müller, R. Kötz, and S. Stucki, A structural investigation of stabilized oxygen evolution catalysts. *J. Mater. Sci.*, **19**(12) (1984) 3987-3994.

133. E. Rasten, G. Hagen, and R. Tunold, Electrocatalysis in water electrolysis with solid polymer electrolyte. *Electrochim. Acta*, **48**(25–26) (2003) 3945-3952.

134. J. Cheng, H. Zhang, G. Chen, and Y. Zhang, Study of IrxRu1-xO2 oxides as anodic electrocatalysts for solid polymer electrolyte water electrolysis. *Electrochim. Acta*, **54**(26) (2009). 6250-6256.

135. X. Wu, K. Scott, and V. Puthiyapura, Polymer electrolyte membrane water electrolyser with Aquivion® short side chain perfluorosulfonic acid ionomer binder in catalyst layers. *Int. J. Hydrogen Energ.*, **37**(18) (2012) 13243-13248.

136. E. Rasten, Electrocatalysts in Water Electrolysis with Solid Polymer Electrolyte. PhD thesis, Norwegian University of Science and Technology, URN:NBN:no-7264, 2001.

137. J. Cheng, H. Zhang, H. Ma, H. Zhong, and Y. Zou, Preparation of Ir0.4Ru0.6MoxOy for oxygen evolution by modified Adams' fusion method. *Int. J. Hydrogen Energ.*, **34**(16) (2009) 6609-6613.

138. K.M. Papazisi, A. Siokou, S. Balomenou, and D. Tsiplakides, Preparation and characterization of $Ir_xPt_{1-x}O_2$ anode electrocatalysts for the oxygen evolution reaction. *Int. J. Hydrogen Energ.*, **37**(21) (2012). 16642-16648.
139. X. Wu, J. Tayal, S. Basu, and K. Scott, Nano-crystalline RuxSn1-xO2 powder catalysts for oxygen evolution reaction in proton exchange membrane water electrolysers. *Int. J. Hydrogen Energ.*, **36**(22) (2011). 14796-14804.
140. S. Srinivasan, A. Ferreira, R. Mosdale, S. Mukerjee, J. Kim, S. Hirano, S. Lee, F. Buchi, and A. Appleby, Proceedings of the Fuel Cell-Program and Abstracts on the Proton Exchange Membrane Fuel Cells For Space And Electric Vehicle Application. p. 424-427, 1994:
141. M.S. Wilson, J.A. Valerio, and S. Gottesfeld, Low platinum loading electrodes for polymer electrolyte fuel cells fabricated using thermoplastic ionomers. *Electrochim. Acta*, **40**(3) (1995) 355-363.
142. S. Gottesfeld and M. Wilson, Thin film catalyst layers for polymer electrolyte fuel cell electrodes. *J. Appl. Electrochem.*, **22 (**1992) 1-7.
143. E. Gülzow, M. Schulze, N. Wagner, T. Kaz, R. Reissner, G. Steinhilber, and A. Schneider, Dry layer preparation and characterization of polymer electrolyte fuel cell components. *J. Power Sources*, **86**(1) (2000) 352-362.
144. S. Ardizzone, G. Fregonara, S. Trasatti, *"*Inner" and "outer" active surface of RuO_2 electrodes. *Electrochim. Acta,* **35** (1990) 263-267.

Chapter 4

Zirconium(IV) hydrogenphosphate as an additive in electrocatalytic layers for the oxygen-evolution reaction

A. Zlotorowicz, F. Seland, S. Sunde

Department of Materials Science and Engineering, Norwegian University of Science and Technology, N-7491 Trondheim, Norway

4.1 Abstract

Composite thin-film electrodes of iridium oxide, zirconium(IV) hydrogenphosphate, and Nafion were fabricated on glassy carbon working electrodes. The performance of the electrodes for the oxygen-evolution reaction depends critically on the way the composite electrodes are manufactured. Application of phosphoric acid in the synthesis of the zirconium(IV) hydrogenphosphate can be detrimental to the catalytic activity, unless synthesis conditions assure complete reaction of phosphoric acid with the other reactants (zirconium oxychloride). Zirconium oxychloride was not found to be adversely affecting the catalyst. The resulting zirconium(IV) hydrogenphosphate does also to some extent block the catalyst surface. Therefore, for high-temperature applications the amount of zirconium(IV) hydrogenphosphate in catalytic layers must be carefully optimised for optimum combination of performance and mechanical properties.

Is not included due to copyright

Chapter 5

Composite thin film iridium-niobium oxide electrocatalysts for the oxygen evolution electrode

A. Zlotorowicz, F. Seland, S. Sunde

Department of Materials Science and Engineering, Norwegian University of Science and Technology, N-7491 Trondheim, Norway

5.1 Abstract

A series of $(IrO_2)_{1-x}(Nb_2O_5)_x$ catalyst with Nb_2O_5 loading from 0.1-0.7 mol% was prepared by hydrolysis method and annealed at 500 ºC. Electrodes of the catalyst powder was characterized in 0.5 mol dm^{-3} H_2SO_4 by cyclic voltammetry (CV) and quasi steady-state polarisation measurements (LSV). X-ray diffraction (XRD) and X-ray photoelectron spectroscopy (XPS) indicated a phase separation into iridium oxide and niobium pentoxide in the catalyst for all compositions and forms composite oxide rather than a solid solution. In line with this, at room temperature the catalytic activity decreased with increasing niobium content in the catalyst. However, raising the temperature to 80 ^{o}C inverted this sequence so that the catalytic activity increased in the order IrO_2 < $(IrO_2)_{0.9}(Nb_2O_5)_{0.1}$ < $(IrO_2)_{0.7}(Nb_2O_5)_{0.3}$.

Is not included due to copyright

Chapter 6

CeO_2 as an additive for anode catalyst of IrO_2 and $Ir_xRu_yO_2$ for PEM water electrolysis

A. Zlotorowicz, F. Seland, S. Sunde

Department of Materials Science and Engineering, Norwegian University of
Science and Technology, N-7491 Trondheim, Norway

6.1 Abstract

The applicability of CeO_2 as an addictive anode with iridium oxide and iridium ruthenium anode catalyst for Polymer Electrolyte Membrane Water Electrolysis (PEM WE) was investigated. The powder catalysts were prepared by hydrolysis method. The morphology of the particle was characterised by the XRD and SEM. Electrodes were characterised in acid solution and water by the cyclic voltammetry and sweep linear voltammetry at various temperatures. The results showed that in acid solution at 80 ^oC the ceria improves the stability and the catalytic activity increased in order $(Ir_{0.8}Ru_{0.2}O_2)_{0.2}(CeO_2)_{0.2}$> $(IrO_2)_{0.7}(CeO_2)_{0.3}$> IrO_2 $\geq$ $(IrO_2)_{0.9}(CeO_2)_{0.1}$. In PEM WE at 80 ^oC ceria causes instability of ruthenium. However ceria with iridium oxide can be used as a catalyst for PEM WE if the CeO_2 content is kept below 10 mol%.

Is not included due to copyright

Chapter 7

Performance of a PEM water electrolysis cell of Ir-based oxide electrodes containing Nb, Ta and Ru for oxygen evolution reaction at 150 ^{o}C

A. Zlotorowicz[a], N. Shroti[b], F. Seland[a], S. Sunde[a], D. K. Niakolas[b],

S. Neophytides[b]

[a] Department of Materials Science and Engineering, Norwegian University of Science and Technology, N-7491 Trondheim, Norway
[b] Foundation for Research and Technology, Hellas Institute of Chemical Engineering Sciences. FORTH/ICE-HT, Greece

7.1 Abstract

The development of proton exchange membrane water electrolysis (PEM WE) requires satisfactory membrane electrode assembly (MEA). TPS membranes doped with phosphoric acid and different catalysts of IrO_2 based oxide with Nb, Ta and Ru were investigated to prepare high performance binder-free MEAs at 150 ºC and at atmospheric pressure. Large differences in the stability of the various catalysts employed were observed, and appear to be potential dependent. Although effects of leakages of phosphoric acid cannot be ruled out, this indicates that the performance loss is associated with catalyst degradation rather than catalyst contamination by phosphoric acid.

Is not included due to copyright

Chapter 8

Conclusions

8.1 Characterisation of zirconium(IV) hydrogenphosphate as an additive in electrocatalytic layers

The main conclusions are:

- Excess of phosphoric acid gives the lowest rate of the oxygen evolution reaction.
- Phosphoric acid tends to block the surface not only for the OER, but also for the exchange of protons.
- Zirconium oxychloride was not found to adversely affect the catalyst.
- Zirconium(IV) hydrogenphosphate in Nafion will lead to some reduction in performance, presumably blocking the catalyst surface.
- In presence of phosphoric acid and zirconium (IV) hydrogenphosphate, the results indicate that the surface can be thought of as consisting of three different parts:
    - completely blocked by phosphoric acid
    - blocked only for the OER
    - open to both proton exchange and the OER.

8.2 Characterisation of iridium-niobium oxide electrocatalysts

The main conclusions are:

- Iridium-niobium oxide electro catalysts synthesised by the hydrolysis method has two separate oxide phases: IrO_2 and Nb_2O_5.

- An addition of Nb_2O_5 to IrO_2 particles had a highly beneficial effect on the catalytic activity at increased temperature in acid solution as compared to the intrinsic IrO_2.
- In addition Nb_2O_5 improves the stability of IrO_2 without appreciable loss of electrocatalytic activity.
- Even addition of 30 mol% Nb_2O_5 in IrO_2 shows a beneficial effect at higher temperature as compared to intrinsic IrO_2 in sulphuric acid solution and also in a PEM WE cell.
- Iridium-niobium oxide is a promising candidate for the oxygen evolution reaction for proton exchange membrane water electrolysers operating at elevated temperatures.
- Better of utilization of IrO_2 was achieved for PEM WE at 80 ºC.

8.3 Characterization of iridium-cerium oxide and iridium-ruthenium-cerium oxide electrocatalysts

The main conclusions are:

- Iridium-cerium oxide electrocatalysts synthesised by the hydrolysis method has two separated oxide phases: IrO_2 and $CeO_{2.}$
- Iridium-ruthenium-cerium oxide electro catalysts synthesised by the hydrolysis method has two separated oxide phases: $IrRuO_2$ and $CeO_{2.}$
- At elevated temperature in sulphuric acid solution, addition of ceria to iridium oxide particles shows a beneficial effect even at 30 mol% ceria relative to intrinsic IrO_2.
- A composite electrode with ceria improves the utilization of iridium oxide and improves anodic stability.
- For PEM WE at room temperature, addition CeO_2 to IrO_2 improves the performance.
- In aqueous solution at 80º C a mixture of cerium and iridium-ruthenium oxide exhibited similar OER activity to that of pure IrO_2 and a mixture of 10 mol% ceria with iridium oxide.
- The amount of ceria in the catalyst should be limited to some 10 % before a significant loss in activity would result.

8.4 Performance of a PEM water electrolysis cell of Ir-based oxide electrodes containing Nb, Ta and Ru with TPS membrane at 150 ºC

The main conclusions are:

- The cross section of the MEA before and after the experiment shows that there is a good contact between the elctrocatalyst and the membrane.
- The thickness of catalysts layer and the membrane after experiments were reduced probably because of loss of catalyst during operation.
- An increase of the potential up to 1.7 V at 150 ºC reduces the active surface area of the electrocatalysts. The stability of high-temperature PEM WE is an issue requiring attention for optimisation of high-temperature PEM WE.
- Phosphoric acid may leak out of the cell during operation, which may imply a loss of proton conductivity at high temperature (and potential).
- 10 mol% niobium oxide in iridium oxide shows higher electrocatalytic activity than the intrinsic IrO_2.
- Addition niobium oxide to iridium improved anodic stability at high temperature (150 ºC).

Chapter 9

Suggestions for further work

9.1 Development of electrocatalysts

Despite the fact that iridium and ruthenium oxides are still the most active catalysts for PEM water electrolysis, they are very expensive and they are less stable at high temperatures. A good solution to reduce costs, improve the activation of the surface area and increase the stability at high temperature is to synthesis the electrocatalyst with a second element.

In our work, iridium niobium oxide improved stability and increased the activity. Also, iridium-niobium oxide is a more promising candidate than iridium-cerium oxide; We therefore suggest developing and continuing the research with niobium mixture to improve stability of the oxides. Suggested approaches might be:

- Synthesis iridium-niobium oxide using the polyol method. This can help to control the particles size, and might also lead to a solid solution. In any event we would expect it to lead to a different morphology.

- Extend investigations whether doping of iridium-ruthenium oxide or ruthenium oxide with Nb_2O_5 may improve the stability of this oxide as well.

Additional characterisation by methods not employed here, e.g. electrochemical impedance spectroscopy can be useful for future work, in particular relating to the conductivity of the oxides. Transmission electron microscope (TEM) is strongly suggested to provide morphological, compositional and crystallographic information on the electrocatalyst powder. Theoretical investigations such as density-functional theory are increasingly important in catalysis research, and have been employed also for water electrolysis catalysts. These could be utilised to probe the possibility of obtaining a solid solution of for example niobium and ruthenium oxide, and whether there would be a stability and activity gain from this.

9.2 Development of the cell for the autoclave

We established the autoclave with the glass pipe, which plays role as a working electrode in the half cell. The construction of the cell is useful to characterise the electrocatalysts up to 200 ˚C. All experiments in this work were performed in acidic solutions. However, it is possible to work with MEAs in liquid electrolytes employing the setup designed. In this way electrocatalytic layers can be conveniently studied without the use of a more complicated test stations. For example, transport properties in the MEA as a function of the amount of ionomer in the layer is one area for which this technique can be used. In fact, such measurements were attempted here, but were not concluded due to leakages in the cell. However, future developments should easily circumvent this problem with further development of gaskets and sealing and the design itself.

9.3 PEM water electrolysis cell

First of all, preparation of the catalytic layer can be improved, for example through use of the autoclave setup as indicated in the previous section. The way the ink is prepared and deposited can be studied. At low temperature of PEM WE Nafion solution is used as a binder to prepare a thin catalytic layer. In the literature we find that there is a gap in terms of studies of the use of ionic conducting binders at high temperature. Zirconium(IV) hydrogenphosphate with Nafion was investigated, and we suggest to use it also as a binder for better ion conducting and additional utilization of the catalyst.

In addition, zirconium hydrogenphosphate with Nafion can act as a barrier between the catalyst and a phosphate-doped membrane to avoid any contamination of the catalyst by phosphoric acid.

Acronyms

AWE	Alkaline Water Electrolysis
BP	Biopolar Plates
CCB	Catalyst covered back
CCM	Catalyst covered membrane
CE	Counter electrode
CV	Cyclic Voltammetry
DHE	Dynamic hydrogen electrode
DSA	Dimensionally Stable Anodes
FEP	Fluorinated ethylene propylene copolymer
GC	Glassy carbon
GDL	Gas diffusion layer
IEP	Isoelectric point
LSV	Linear Sweep Voltammetry
MEA	Membrane electrode assembly
MPL	Micro- protetctive layer
NHE	Normal hydrogen electrode
OER	Oxygen evolution reaction
ORR	Oxygen reduction reaction
PBI	Polibenzimidazol
PEM	Polymer exchange membrane
PEMFC	Proton exchange membrane fuel cell
PEMWE	Proton exchange membrane water electrolysis
PTEF	Polytetrafluoroethylene
pzc	Point of zero charge
RDE	Rotating disc electrode
RE	Reference electrode
RT	Room temperature
SEM	Scanning electron microscopy
SOEC	Solid oxide electrolysis cell
SPEEK	Sulfonated polyetherketone
SPE	Solid polymer electrolyte
WE	Working electrode
ZrP	Zirconium hydrogenphosphate
XPS	X-ray photoelectron spectroscopy
XRD	X-ray diffraction

Errata

page	Incorrect
109	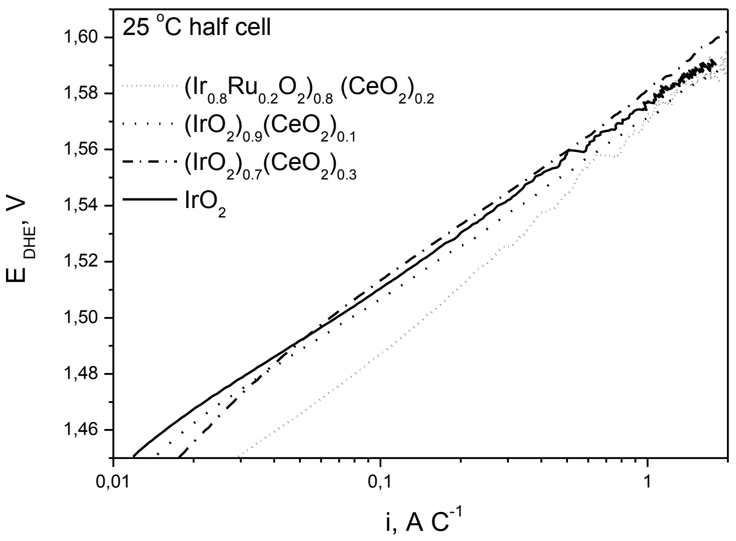
	Correct 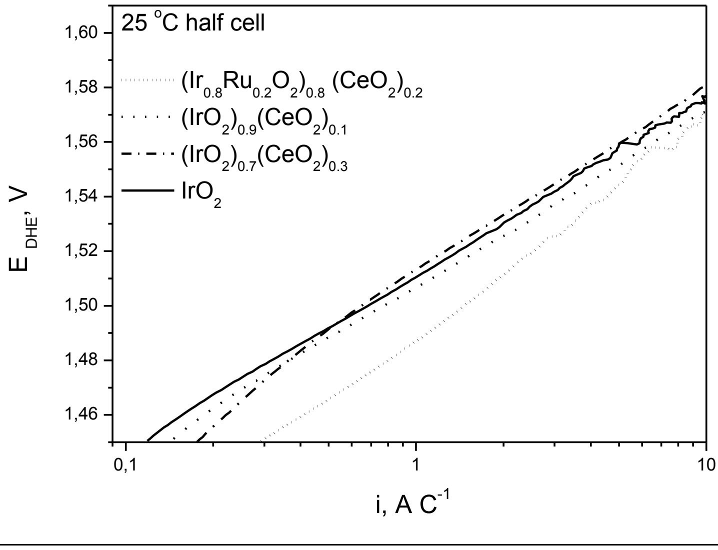 25 °C half cell 1,60 1,58 1,56 1,54 1,52 1,50 1,48 1,46 $(Ir_{0.8}Ru_{0.2}O_2)_{0.8}$ $(CeO_2)_{0.2}$ $(IrO_2)_{0.9}(CeO_2)_{0.1}$ $(IrO_2)_{0.7}(CeO_2)_{0.3}$ IrO_2 E_{DHE}, V 0,1 1 10 i, A C^{-1}